

Search for emission-line galaxies towards nearby voids. Observational data^{*}

Cristina C. Popescu^{1,4}, Ulrich Hopp^{1,2}, Hans Jürgen Hagen³, and Hans Elsässer¹

¹ Max Planck Institut für Astronomie, Königstuhl 17, D-69117 Heidelberg, Germany

² Universitätssternwarte München, Scheiner Str.1, D-81679 München, Germany

³ Hamburger Sternwarte, Gojenbergsweg 112, D-21029 Hamburg, Germany

⁴ The Astronomical Institute of the Romanian Academy, Str. Cuștitul de Argint 5, 75212, Bucharest, Romania

Received 18.08.1995; accepted 12.09.1995,

Abstract. We present the observational results of our search for emission-line galaxies (ELG) towards nearby voids. In order to find ELG, we started a survey using the IIIa-J objective prism plates from the Hamburg QSO Survey. The plates are digitized and an automatic procedure was applied to select the candidates. Digitized direct plates were used to determine coordinates and to reject overlaps between spectra. The accuracy of the coordinates is $\pm 2''$. A total area of 1248 deg^2 was scanned, distributed in four different regions.

All the selected objects were observed with follow-up spectroscopy. We have obtained a final sample of 203 objects, of which 196 are emission-line galaxies, four are galaxies with absorption lines and three are QSOs. Almost half of our objects are newly discovered ones and three quarters of the given redshifts are new. Our sample contains mainly high ionization galaxies and is less sensitive in the detection of low-ionization objects.

The apparent magnitudes, as derived from the objective prism plates, range between $15.0 \leq B \leq 19.5$. The sample is dominated by nearby galaxies, with a peak in the redshift distribution at $cz=4500 \text{ km/s}$.

Key words: large scale structure - galaxies -redshift survey

1. Introduction

Recent redshift surveys of galaxies (e.g. the Center for Astrophysics Survey (CfA)), revealed that bright galaxies are distributed in sheet-like structures which surround large voids. This has been a subject of intense investigation since the proposal of such structures by Zeldovich et al. (1982). Still under debate is the question whether all galaxies follow this non-uniform distribution or if less luminous galaxies are more equally distributed. Given the limitation of the actual surveys, the observed emptiness of the voids may be a result of observational bias. From an observer's point of view, the galaxy maps may

reflect special observational selection effects in surface brightness, integral magnitude or diameter. From the theoretical point of view, there has been the prediction (e.g. Kaiser 1986, Bardeen 1986) that luminous galaxies were formed preferentially in high-density regions of the Universe, thus giving us a biased view of the large-scale distribution of matter.

Several studies of the spatial distribution of galaxies, especially of dwarf galaxies, were carried out to overcome some of these biases (e.g. Binggeli et al. 1990, Thuan et al. 1991). Unfortunately the results were contradictory and no definitive conclusions were drawn. Some interesting results came from the study of the spatial distribution of emission-line galaxies (ELG) (Salzer 1989, Weistrop et al. 1992). These objects are intrinsically small, very compact and with low luminosities. In some cases they are so compact that they look almost stellar, with no obvious underlying galaxy. Such galaxies can easily be missed by surveys that select their candidates on morphological criteria or discriminate stars from galaxies by the apparent diameter of the latter, and thus are good candidates to fill up the voids. HII galaxies can be recognised because of their typical emission-line spectrum and an efficient way to find them is to use objective prism plates.

We therefore started a project to search for ELG towards nearby voids, using an objective prism survey. This project belongs to a larger one, that has the aim of finding faint galaxies within the voids (Hopp and Kuhn 1995, Hopp et al. 1995). Previous results on this project showed that while the central part of the voids remains free of galaxies, some of the dwarfs populate the outskirts of the voids. Most of these dwarfs are emission-line galaxies.

During the last two decades much effort has been spent to discover large samples of ELG. One method is to use multiple exposures on the same plate through different filters and search for UV excess objects, as was done by the Kiso UV-Excess Galaxy Survey (Takase and Miyauchi-Isobe 1988) and the Montreal Blue Galaxy Survey (Coziol et al. 1993, Coziol et al. 1994). A second method is to use low resolution objective prism Schmidt plates and search for galaxies with strong UV-continuum. This method was used by Markarian (1967) for the First Byurakan Spectral Sky Survey. Perhaps the most unambiguous method is to use objective prism surveys and search directly for the presence of emission-lines.

Send offprint requests to: Cristina C. Popescu

^{*}Partly based on observations obtained at the European Southern Observatory, La Silla, Chile

Haro (1956) was the first to show that moderate-dispersion plates can show emission-lines of [OII], [OIII], the Hydrogen Balmer series and other elements. The method was successfully applied by Smith (1975) for the Tololo Objective Prism Survey (see also Smith et al. 1976, Bohuski, Fairall and Weedman 1978). They used the 61-cm Curtis Schmidt telescope at Cerro Tololo to take IIIa-J (1740 Å/mm at $H\beta$) plates. The same technique was then applied for the University of Michigan Survey (UM) (MacAlpine et al. 1977a,b,c, MacAlpine & Lewis 1978, MacAlpine & Williams 1981), the Calan-Tololo Survey (Maza et al. 1989), the Wasilewski Survey (Wasilewski 1983), and the Surace & Comte Survey (Surace 1993, Surace & Comte 1994). Sometimes a combination between emission-line and UV-excess criteria was applied, as in the Case Survey (Sanduleak & Pesch 1982, 1984, 1987, 1989, 1990, Pesch & Sanduleak 1983, 1986, 1988, 1989, Pesch et al. 1991, Stephenson & Pesch 1992, Pesch et al. 1995). An alternative to the IIIa-J plates is to use red IIIa-F objective plates to search for $H\alpha$ emission-lines. These surveys seem to be complementary to the IIIa-J surveys, as discussed by Zamorano et al. 1994. The main $H\alpha$ surveys were: Wamsteker et al. 1985, Moody et al. 1987, and Universidad Complutense de Madrid Survey (UCM) (Zamorano et al. 1990, 1994, Gallego 1995). Smaller areas of sky were searched by Kunth et al. 1981 (two IIIa-F plates) and Kunth & Sargent 1986 (three IIIa-J plates in the Sculptor Region). A combination between both IIIa-J and IIIa-F plates was used by Kinman (1984). Finally, the Second Byurakan Spectral Sky Survey (SBSS) (Markarian et al. 1983a,b, 1984, Stepanian et al. 1990, 1991), which is in progress, observed each field in three different colours: UV and blue region (IIIa-J plates), green region (IIIa-J + GG495) and red region (IIIa-F plates + RG2).

Despite the long lists of candidates that were produced, most of these surveys did not undertake systematic and complete follow-up spectroscopy of their candidates. The most complete and deep sample of ELG remains probably the Michigan Survey. For UM List IV and List V, a sample with complete follow-up observations was obtained (Salzer et al. 1989). A similar sample was obtained for List I and List II of the Case Survey (Salzer et al. 1995). On the other side, most of these surveys searched by eye their candidates and thus cannot provide objective selected samples. Modern techniques for the digitization of Schmidt plates, as pioneered in Cambridge (Kibblewhite et al. 1984; Irwin & Trimble 1984) or Edinburgh (Cooke et al. 1986), now offer the possibility of performing the object searches using controlled selection criteria. These techniques were already used for QSO searches (Clowes et al. 1984; Hewett et al. 1985, Wisotzki 1994, Hagen et al. 1995). The Surace & Comte Survey is the first survey for ELG that selected their candidates using digitized plates. Details of the digitized procedure are given in Surace & Comte 1994 (see also Surace 1995). The UCM survey applied a digitized procedure in order to test their eye selected sample (Alonso 1995).

A new era in the survey techniques was opened by the use of grisms and CCD cameras as detectors (e.g. Palomar Transit Grism Survey, Schneider et al. 1994). While these kind of surveys have the advantage of going deeper, their small field of view makes the photographic plate surveys still competitive when covering wide fields.

In this paper we present an objective prism survey that used digitized plates and an automatic procedure to search for ELG candidates. All the objects selected from the plates

were observed with follow-up spectroscopy, thus providing a complete sample of emission-line galaxies. The paper describes the selection of the sample and the follow-up observations. The study of the spatial distribution of our sample of emission-line galaxies, as well as their properties, will be given elsewhere.

The paper is organized as follows. In § 2 we describe the method used to select the candidates from the objective plates. In § 3 the follow-up spectroscopy is presented, in § 4 we discuss the results of our survey and § 5 contains the conclusions.

2. Selection of candidates on objective prism plates

We used published cone diagrams to identify nearby ($v_R \leq 7500 \text{ km/s}$) voids. Four void regions were selected according to the following criteria: diameter larger than 20 Mpc ($H_0 = 75 \text{ km/s/Mpc}$), completely empty of CfA galaxies, galactic latitude $b \geq 30^\circ$. The location of the four void regions can be found in Table 1, where we give the exact coordinates of all the fields surveyed.

The ELG candidates were selected on the objective prism plates taken in the frame of the Hamburg Quasar Survey (HQS) (Hagen et al. 1995). The plates are taken with the 80-cm Schmidt-telescope at the German-Spanish Observatory, Calar Alto (Spain). The telescope is equipped with a 1.7° objective prism producing a dispersion of 1390 Å/mm at $H\gamma$. The $24 \text{ cm} \times 24 \text{ cm}$ hypersensitized Kodak IIIa-J plates (spectral range: 3400 Å-5500 Å), covering a field of $5.5^\circ \times 5.5^\circ$, were scanned with low resolution (LR), using a PDS 1010G microdensitometer. The LR mode used a $100 \mu\text{m}$ slit running perpendicular to the direction of dispersion. After on-line background reduction and object recognition, LR spectra were stored on optical disks. Automated search software was applied to the LR digitized data to select spectra in a specific parameter space. The two parameters used were the density sum of intensity (“brightness”) of the integrated spectra and the slope of the continuum (“colour”), which is again a function of the density sum. Brighter objects are redder because the sensitivity of the photographic plate increases with wavelength. The selected spectra were re-scanned individually with high resolution (HR) ($30 \mu\text{m}$ slit) and the final digitized spectra were visually inspected for emission lines.

The range in density sum excludes very bright objects, that are not needed for our study, but also very faint objects, that lie very close to the detection limit of the plate. The limit at the very bright end helps us to decrease the number of uninteresting candidates, while bright galaxies (brighter than our threshold) with emission are still found due to their HII regions. These knots are found as individual objects and their brightnesses are therefore fainter than those of the underlying galaxies. Nevertheless, these bright galaxies are already known and contained in galaxy catalogs like the CfA. The incompleteness due to the faint limit in the low-density region was analyzed as follows. For three plates we extended our search to the very faint end (which is only 20% of the whole range used), and we found twice (or even more) as many candidates as in the normal range. Most of these extra spectra were very noisy and could not be classified. Thus the efficiency of finding interesting objects was rather reduced and the number of objects and the quality of the spectra depended more strongly on plate quality. Our tests showed that we can miss some faint emission-line galaxies, on the order of 2 per plate (0.06 deg^{-2}), but one can correct for these numbers. Due to our automated

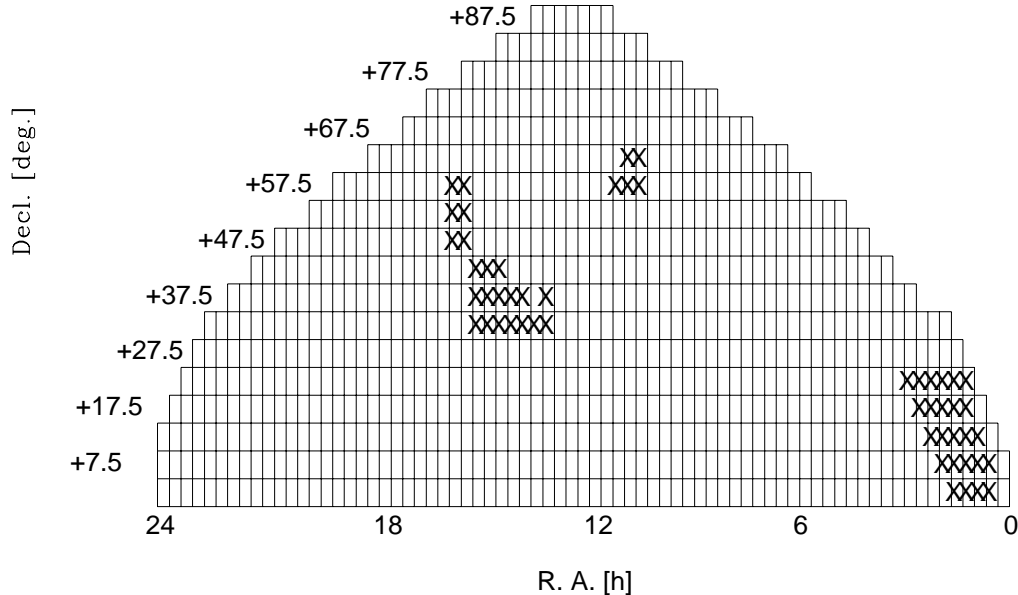


Fig. 1. The map of the Northern Sky, divided into fields of $5.0 \times 5.0 \text{ deg}^2$. We marked with crosses the plates that were inspected in our ELG Survey. Each plate covers a field of $5.5 \times 5.5 \text{ deg}^2$, thus allowing an overlap between neighbour plates of 0.5° . Field centres are provided in Table 1.

search software, the incompleteness at the very faint end of the “brightness” parameter can be quantified. The other parameter, the slope of the continuum, is set so that only the bluest objects are selected. To do this we estimate the slope as a function of density sum, and for each bin of density sum, a fraction $f=0.15$ of the bluest objects are considered. The colour selection causes our sample to be dominated by very blue galaxies. In order to test this selection effect, we searched two plates without any restriction in the colour parameter. Our tests showed again that we can miss some emission-line galaxies that are redder than our selection criteria. These galaxies are usually strong emission-line objects and have also strong continua, that is produced by an underlying older population of stars. As we are more interested in dwarf emission line galaxies, we believe that our blue criteria help us to select a sample

that is less contaminated by other kinds of emission-line galaxies. We will refer to our selection criteria as the blue criteria, though it includes a selection in a two parameter space.

The number of candidates for high resolution varies between 1500 and 3500 per plate, depending on the plate quality and on the galactic latitude. Those HR spectra which show strong $[\text{OIII}]\lambda 5007$ lines are selected the final sample of candidates. The $[\text{OIII}]$ line appears as a distinctive peak near the green head of the objective prism spectra. Often the $[\text{OII}]\lambda 3727$ doublet can be identified too. Some typical HR objective prism spectra are given in the left panels of Fig. 4. The aim of the Hamburg Survey is to cover every Schmidt field with two plates, in order to allow the distinction between real emission-lines and plate defects. Unfortunately the regions we scanned were not always covered by two plates, as the Hamburg sur-

Table 1. The coordinates of the centre of the plates that were scanned in our ELG Survey. The first column gives the void region (from 1 to 4) for which the plates were selected

1	$\delta = 2.5^\circ: \alpha = 00^h 20^m; 00^h 40^m; 01^h 00^m; 01^h 20^m;$ $\delta = 7.5^\circ: \alpha = 00^h 20^m; 00^h 40^m; 01^h 00^m; 01^h 20^m; 01^h 40^m;$ $\delta = 12.5^\circ: \alpha = 00^h 20^m; 00^h 41^m; 01^h 01^m; 01^h 21^m;$ $01^h 41^m;$ $\delta = 17.5^\circ: \alpha = 00^h 21^m; 00^h 42^m; 01^h 03^m; 01^h 23^m;$ $01^h 44^m;$ $\delta = 22.5^\circ: \alpha = 00^h 00^m; 00^h 21^m; 00^h 43^m; 01^h 04^m;$ $01^h 26^m;$
2	$\delta = 57.5^\circ: \alpha = 08^h 12^m; 08^h 47^m; 09^h 22^m;$ $\delta = 62.5^\circ: \alpha = 08^h 00^m; 08^h 40^m;$
3	$\delta = 32.5^\circ: \alpha = 13^h 10^m; 13^h 33^m; 13^h 56^m; 14^h 19^m;$ $14^h 43^m;$ $\delta = 37.5^\circ: \alpha = 12^h 37^m; 13^h 25^m; 13^h 50^m; 14^h 14^m;$ $14^h 39^m; 15^h 03^m;$ $\delta = 42.5^\circ: \alpha = 14^h 24^m; 14^h 50^m; 15^h 16^m;$
4	$\delta = 47.5^\circ: \alpha = 16^h 00^m; 16^h 28^m;$ $\delta = 52.5^\circ: \alpha = 16^h 42^m; 17^h 13^m;$ $\delta = 57.5^\circ: \alpha = 16^h 59^m; 17^h 34^m;$

vey is still in progress. For the fields where we had to rely on only one plate, the success rate of our selection (see below) is lower because of the addition of a few false candidates that did not show any emission lines in the follow-up observations. Also there were not always high quality plates available for every field. The final sample contains 234 candidates, distributed in four different regions, in a total scanned area of 1248 deg^2 . With a surface density of $0.19 \text{ candidates/deg}^2$, we will refer to this sample as the first priority sample. In Fig. 1 we show the map of the scanned fields. In Table 1 we give the coordinates of the centre of the corresponding plates, separate for every void region. One plate covers a field of $5.5^\circ \times 5.5^\circ$ and there is an overlap between neighbour plates of 0.5° .

Though our main selection criteria was the presence of emission features, we have also second priority candidates that were chosen because of their very blue continuum. With a surface density of about $1 \text{ candidate/deg}^2$, these objects do not show any reliable emission features and for this reason they were considered as a separate sample.

Digitized direct plates were used to determine coordinates, to reject artificially blue objects created by overlaps of two spectra, and finally to produce finding charts. For details of the digitization procedure and astrometric determinations see Hagen et al. (1995).

3. Follow-up spectroscopy

We observed our candidates during several observing runs, most of them being carried out with the 2.2 m telescope at the German-Spanish Observatory at Calar Alto (Almeria, Spain).

Table 2 lists the dates of the different runs, as well as the instruments and particularities of the set-up used each time.

At the 2.2 m telescope in Calar Alto we used a Boller & Chivens standard spectrograph (runs: 2,4,7) and also the new CAFOS (Calar Alto Faint Object Spectrograph) focal reducer system and grisms (run 3). A few observations were made with the Prime Focus Focal Reducer at the Calar Alto 3.5 m telescope. Runs 1 and 6 were not dedicated to our project, therefore our candidates (only 8) were observed as backup objects. During all the Calar Alto observations, a Tektronix 1024 by 1024 24μ pixel size CCD chip served as the detector while a coated Thompson 1024 by 1024 19μ chip was used at La Silla (run 6). In all cases, a long slit of about 2 arcsec width was used. With the focal reducers, we always obtained a blue and/or a red image which served for the measurements of magnitudes and to estimate morphological types. The usual calibration measurements (bias-and flat-frames for the CCD correction, wavelength calibration frames and flux standard stars) were carried out.

Typical exposure times were 10-15 minutes, depending primarily on the strength of the emission-lines: strong-line objects were not observed as long as weaker line galaxies. The exposure time depends also on the brightness of the galaxy, though not so strongly. For example, for very faint objects with almost no underlying continuum but with strong emission features, an integration of 10 minutes brought enough fluxes in the emission lines to properly reduce the spectrum. By contrast, brighter objects, with strong continuum but very weak lines (or no obvious emission features in the objective spectra) had to be integrated longer.

The frames were biased and flatfield-corrected. For the extraction of the 1-dimensional spectra from the 2-dimensional data, the optimal extraction algorithm of Horne (1986) was used. The spectra were rebinned to a linear wavelength scale using a third or fifth order polynomial fitted to the dispersion curve of the comparison spectra. A flux calibration was applied, and finally the wavelength scale was checked by comparison with the night-sky lines. A more detailed description of the reduction procedure is given by Stickel et al. (1993).

Once fully reduced, the emission lines in each spectrum were measured by fitting a Gaussian. The quoted redshifts were derived as means of the redshifts determined from the individual strong lines, and the errors of the redshifts were calculated as error of the mean. The observed redshifts were further corrected for the motion of the Earth and transformed in heliocentric redshifts. The calculated errors were compared with the deviations obtained from the night-sky line measurements. We estimate that for the spectra taken in the runs 3,4,7, which consist of 85% of our data, the errors are $\Delta z=0.0001$. This value can increase up to $\Delta z=0.0002$ for some of the galaxies with very noisy spectra. For the rest of our spectra (15%) the errors are bigger, up to $\Delta z=0.0005$. During run 7, some planetary nebulae with known redshifts were observed (NGC6543, NGC0040, NGC1501, NGC2022, NGC2392, PN212.0), in order to check the quality of our wavelength calibration. The reference values of the planetaries were taken from The Strasbourg-ESO Catalogue of Galactic Planetary Nebulae. (Acker et al. 1992)

In Fig. 2 we plotted the observed velocities versus the reference velocities and applied a linear fit. As one can see, the differences between our velocities and those from literature are in the range of the assumed errors. We obtain a correlation

Table 2. Dates and set-up of the spectroscopic observations: BCCS: Boller & Chivens Cassegrain Spectrograph, CAFOS 2.2 : Calar Alto Faint Object Spectrograph at the 2.2 m telescope, PFFR: Prime focus focal reducer, EFOSC2: ESO Faint Object Spectrograph and Camera 2, CA: Calar Alto, LS: La Silla

No.	Dates	Telescope	Instrument	Spectral Range (Å)	Spectral Resolution (Å)
1	1994 Jan 2-3	2.2 m CA	BCCS	3600-6500 6200-9000	6.5 6.5
2	1994 Jan 4-9	2.2 m CA	BCCS	3700-9000	17
3	1994 June 8-11	2.2 m CA	CAFOS 2.2	3900-8200	18
4	1994 Oct 9-12	2.2 m CA	BCCS	3600-9000	12
5	1994 Oct 13	3.5 m CA	PFFR	3500-7600	20
6	1994 Dec 10	2.2 m LS	EFOSC2	3500-5500	12
7	1995 Jan 31- Feb 3	2.2 m CA	BCCS	3460-8600	12

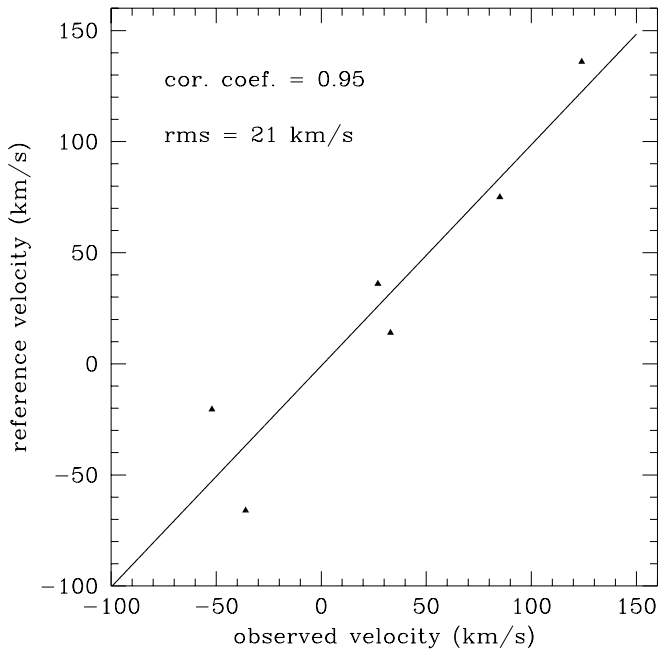


Fig. 2. The observed velocities of the planetary nebulae used to check the redshift errors, versus their reference velocities. A linear fit is applied to the data points and a correlation coefficient of 0.95 is obtained.

coefficient of 0.95 and a rms of 21 km/s, in agreement with our expectations.

A further test came from the observations of some candidates that had redshifts given in the literature. In Table 3 we give the names of the galaxies observed together with their velocities, both measured and from the literature. In the last

Table 3. Candidates with available redshifts from literature, observed with the purpose of testing the redshift accuracy.

name	our redshift	reference redshift	difference in redshift
CG 0419	0.0114	0.0114	0.0000
DDO 166	0.0031	0.0032	0.0001
UM 065	0.0210	0.0210	0.0000
DDO 13	0.0021	0.0021	0.0000
UM 306	0.0170	0.0164	0.0006

column we indicate the difference between our values and the reference ones. These galaxies were measured during the runs for which we estimated an error of 0.0001 in z . Besides UM 306, for which we obtained a big difference, the rest show differences of about 0.0001. In order to see if the estimated error of 0.0001 in z is constant through all the runs where we assumed such an error, we observed a few candidates twice, in different runs. The results of these tests indicate that the errors do not change with the run.

Before starting the observations, we checked our lists of candidates with the present catalogs of galaxies and emission-line objects, in particular with the NASA Extragalactic Data Base (NED). Candidates found by other surveys with available redshifts were normally not reobserved. There were cases in which the candidates were contained also in other catalogs, but with unknown redshifts. We observed these, together with the newly discovered objects. All first priority candidates with unknown redshifts (182 out of 234) were measured and also some of our second priority ones (83). The latter were observed to test their nature and we did not intend to be complete with these objects. From the observed 182 first priority candidates, 126 showed emission lines, the rest being failures (either featureless spectra or stars). If we consider the whole sample of

254 first priority candidates (52 were objects found already in the literature with available redshifts), the success rate of our selection is 76%. Some of our failures come from the fields covered only by one plate (see § 2). But more important is the dependence of the success rate with the apparent magnitude (see p. 290, Hopp et al. 1995). For brighter objects the success rate is almost 100%, decreasing for the fainter ones.

The observed objects are listed in Table 4, which contains only the objects for which a redshift was assigned (failures not included). Most of our spectra show the emission lines of [OII] $\lambda\lambda 3727$, H $\beta\lambda\lambda 4861$, [OIII] $\lambda\lambda 4959$, [OIII] $\lambda\lambda 5007$, H $\alpha\lambda 6563$ and [SII](blend) $\lambda\lambda 6724$. Many spectra also show the fainter emission lines of ion species like [NeIII], [HeII], [OI], [OII], [AIII], as well as some further Balmer lines, from H γ to H ζ . These are mainly high ionization type spectra, which dominate our sample of ELG. We have even cases with very strong [OIII] $\lambda\lambda 4363$, despite the short exposures that were used to take the spectra. Nevertheless there are also intermediate ionization spectra as well as low ionization ones, the latter coming mainly from the second priority sample. A few cases contain objects in which only H α and [SII] were detected. The spectra with only one line detection (four cases) are marked with an asterisk in Table 4. The table is organized as follow:

- **Column (1)** gives the name of our objects, which is built with the prefix HS (from Hamburg Survey), followed by the first four digits of the 1950.0 right ascension and declination;
- **Column (2)** gives alternate designations for those galaxies contained in other catalogs. The abbreviations are explained in the List of Abbreviations, given at the end of the table.
- **Column (3) and (4)** give the 1950.0 positions. The coordinates are derived from the Hamburg direct plates and have an accuracy of $\pm 2''$. There are few cases in which some HII regions in normal galaxies were found. The coordinates refer then to the position of the HII region rather than to the centre of the galaxy. Special remarks are made for each case.
- **Column (5)** gives the heliocentric redshifts,
- **Column (6)** the B magnitudes as derived from the Hamburg objective prism plates (B_H) and
- **Column (7)** the magnitudes from literature, B_L (where available). For details of the magnitude calibration see Engels et al. (1994). The magnitude accuracy is 0.5^m . Sometimes our magnitudes were fainter than those found in literature, because they refer only to the emission region, and not always to the underlying galaxy.
- **Column (8)** contains a flag S (from selection) that gives the selection criteria used to select the candidates from the objective prism spectra: E for emission candidate (first priority) and B for blue candidate (second priority) (see § 2).
- **Column (9)** contains either the number of the run in which the object was observed (with the prefix o - from observed) or the code of the reference, when the object had available redshift (with the prefix l - from literature). The numbers of the observing runs are the same as listed in Table 2. The codes for references are explained at the end of the table, in the “References to Table 4”.
- **Column (10)** contains special remarks.

Finding charts of all our newly discovered objects can be found in Fig. 3. We also give the finding charts of some of

our objects that were previously known as HCB sources but without any follow-up spectroscopy. The finding charts were prepared by means of the Palomar Sky Survey plates, digitized and distributed on CD-ROM by the Space Telescope Science Institute. Fields are $10' \times 10'$. North is up, and east is to the left.

Some typical examples of our slit spectra are given in the right panels of Fig. 4, while the corresponding HR objective prism spectra can be found in the left panels. In the last slit spectrum, HS0153+2205, the [OIII] line is under the limit of a clear detection, the only lines being the H α +NII. The corresponding objective prism spectrum was very noisy, and what appeared to be an [OIII] line was in fact spurious. We also give the spectrum of a Sy 1 galaxy, HS0814+6439. The identified emission lines are listed in Table 5 while the lengthy discussion of their strength is left for a separate paper. Those objects which are certainly stars are listed in Table 6.

(1)	(2)	(3)	(4)	(5)	(6)	(7)	(8)	(9)	(10)
object name	other names	R.A.	Decl.	redshift	B _H	B _L	S	run or reference	remarks
HS0000+2252	IRAS F00000+2252 NPM1G +22.0001	00 00 01.0	+22 52 20	0.0730	16.3	17.33	E	o4	IrS
HS0000+2422	NPM1G +21.0002	00 00 20.9	+24 22 35	0.0382	17.0		E	o4	IrS
HS0006+2133	IRAS 00067+2133 IRAS F00067+2133 [dKM92] 003	00 06 43.7	+21 33 09	0.0774	17.5	16.9	E	l12	IrS
HS0013+0809		00 13 02.0	+08 09 37	0.0844	19.3		E	o7	
HS0013+1942		00 13 14.4	+19 42 08	0.0258	17.1		E	o4	abs
HS0013+2241		00 13 15.0	+22 41 45	0.0217	17.7		E	o4	
HS0016+1449		00 16 35.7	+14 49 44	0.0147	17.6		E	o7	
HS0020+0656	UM 029	00 20 18.4	+06 56 53	0.051	18.0		E	l77	
HS0021+1347		00 21 50.5	+13 47 33	0.0144	16.5		E	o2	
HS0022+0014	UM 241	00 22 46.1	+00 14 54	0.0139	16.3		E	o4	
HS0022+1945		00 22 44.8	+19 45 23	0.0926	18.2		E	o5	
HS0024+2314		00 24 15.4	+23 14 37	0.0238	18.0		E	o4	
HS0024+1022		00 24 32.2	+10 22 28	0.0071	17.0		E	o2	
HS0026+0332		00 26 52.4	+03 32 49	0.0410	17.5		E	o4	
HS0028+1747		00 28 42.1	+17 47 58	0.0978	18.1		E	o7	
HS0029+1748	NPM1G +17.0024	00 29 26.5	+17 48 11	0.0073	17.5	18.03	E	o7	
HS0029+1443		00 29 42.3	+14 43 38	0.0175	17.2		E	o7	
HS0032+0116	UM 258	00 32 03.3	+01 16 10	0.0147	19.0		E	o7	
HS0033+0421	UGC 00359 UM 048 CGCG 409-047 CGCG 0033.6+0422 MCG +01-02-035 IRAS 00335+0421 IRAS F00336+0421	00 33 36.0	+04 21 37	0.01637	16.5	15.5	E	l19	IrS
HS0035+0725		00 35 45.9	+07 25 29	0.8541	18.3		E	o7	QSO
HS0036+0437		00 36 01.6	+04 37 19	0.0289	17.3		E	o4	
HS0036+0352		00 36 05.7	+03 52 32	0.3884	18.5		E	o5	*
HS0037+0111		00 37 45.2	+01 11 18	0.0136	17.0		E	o4	
HS0038+0122	PC 0038+0122	00 38 06.1	+01 22 52	0.066	17.6	18.11	B	l67	
HS0040+0952		00 40 51.5	+09 52 29	0.0156	17.3		E	o4	
HS0041+2333		00 41 41.3	+23 33 36	0.0218	17.7		E	o4	
HS0043+0531		00 43 16.2	+05 31 37	0.0408	17.6		E	o7	
HS0044+0453	UM 065	00 44 52.8	+04 53 27	0.021	17.2		E	l77	
HS0045+0020	UM 279	00 45 55.6	+00 20 50	0.0381	18.9		E	o7	
HS0049-0006	UM 282 UCM 0049-0006	00 49 13.4	-00 06 33	0.037	19.1	18	E	l77	
HS0049+0017	UM 283 UCM 0049+0017	00 49 15.5	+00 17 38	0.01500	17.0	16.76	E	l58	
HS0051+0927		00 51 22.4	+09 27 27	0.0202	18.9		E	o7	
HS0051+0555	UM 077	00 51 44.4	+05 55 35	0.017	18.6		B	l77	
HS0052+2119		00 52 33.0	+21 19 52	0.0434	17.7		E	o4	
HS0055+0104	UM 293	00 55 19.8	+01 04 04	0.0567	16.8	16.4	E	l13	Sy1.5
HS0056+0044	UM 295 UCM 0056+0044	00 56 21.3	+00 44 09	0.0176	17.2		E	o4	
HS0056+0043	UM 296 IRAS F00564+0043 UCM 0056+0043	00 56 30.0	+00 43 55	0.01800	16.5	16.58	E	l58	IrS

(1)	(2)	(3)	(4)	(5)	(6)	(7)	(8)	(9)	(10)
object name	other names	R.A.	Decl.	redshift	B _H	B _L	S	run or reference	remarks
HS0058+1847		00 58 52.6	+18 47 25	0.0376	17.4		E	o7	
HS0058+0638	UM 082 NPM1G +06.0048	00 58 44.7	+06 38 42	0.051	17.2	17.88	E	l77	Sy 2
HS0101+0310		01 01 24.9	+03 10 56	0.0654	17.3		E	o4	
HS0103+2441		01 03 40.5	+24 41 12	0.0541	17.1		B	o5	
HS0103+1242	IRAS F01037+1242	01 03 46.4	+12 42 29	0.0447	16.5		E	o4	IrS
HS0104+0622	UM 085 NPM1G +06.0054	01 04 09.3	+06 22 00	0.041	17.2	17.29	E	l77	Sy 2
HS0106+1304		01 06 14.5	+13 04 14	0.0597	16.8		E	o4	
HS0107+1946		01 07 29.7	+19 46 38	0.0423	18.0		E	o4	
HS0107+2458		01 07 58.5	+24 58 26	0.0394	17.3		B	o5	
HS0108+0150	UM 306	01 08 00.4	+01 50 52	0.0170	15.9		E	o4	
HS0108+0103	UM 307 UGC 00749 CGCG 385-022 CGCG 0109.0+0104 MCG +00-04-030 IRAS 01089+0103 IRAS F01089+0103	01 08 56.6	+01 03 19	0.0228	17.6	14.31	E	l77	HII region in an Sdm IrS
HS0110+2149	NPM1G +21.0055	01 10 31.6	+21 49 54	0.0563	18.3	16.69	E	o4	
HS0111+1300	UGC 00774 MRK 0975 CGCG 0111.2+1300 IRAS F01112+1300 OC +118	01 11 12.4	+13 00 25	0.0491	16.8	14.76	E	l13	Sy 1 IrS Radio S
HS0111+2115	NPM1G +21.0056	01 11 55.6	+21 15 25	0.0318	16.3	16.42	E	o7	
HS0113+1750		01 13 59.5	+17 50 03	0.0626	18.5		E	o7	
HS0115+1156	MRK 0979	01 15 22.6	+11 56 38	0.0190	15.6	15.5	E	l44	
HS0116+2244	NPM1G +22.0058	01 16 53.0	+22 44 33	0.0439	17.2	16.80	B	o7	abs
HS0117+1017		01 17 13.6	+10 17 33	0.0342	16.5		E	o6	
HS0117+1135		01 17 29.8	+11 35 17	0.0615	16.2		B	o7	
HS0118+1236		01 18 36.4	+12 36 49	0.0198	16.7		E	o6	
HS0119+0331	UM 099	01 19 32.6	+03 31 41	0.0237	16.5		E	o4	
HS0119+0044	IRAS 01197+0044	01 19 43.9	+00 44 42	0.0555	16.9		E	l72	IrS
HS0122+0743	UGC 00993	01 22 57.1	+07 43 47	0.00975	17.6	15.00	E	l19	
HS0123+1624		01 23 36.3	+16 24 55	0.0290	17.2		E	o7	
HS0124+1126	NPM1G +11.0056	01 24 46.4	+11 26 42	0.0327	16.7	17.36	E	o6	
HS0131+1937	IRAS F01318+1936	01 31 52.3	+19 37 04	0.0359	17.6		E	o7	IrS
HS0133+1341		01 33 43.0	+13 41 43	0.0239	17.7		E	o7	
HS0137+1539	UGC 01176 DDO 013 [RC2] A0137+15 LGG 029: [G93] 006	01 37 30.4	+15 39 34	0.0021	18.8	14.4	E	o7	HII region in an Im
HS0138+0458	UM 126	01 38 48.8	+04 58 04	0.032	17.4	18.0	E	l80	
HS0141+0719		01 41 23.4	+07 19 46	0.023	16.3		E	l80	
HS0142+1651	MRK 0361 CGPG 0142.0+1650 [RC2] A0142+16 NPM1G +16.0052	01 42 03.7	+16 51 31	0.0275	15.8	15.6	E	l50	
HS0143+2400		01 43 07.5	+24 00 55	0.0346	18.4		E	o7	

(1)	(2)	(3)	(4)	(5)	(6)	(7)	(8)	(9)	(10)
object name	other names	R.A.	Decl.	redshift	B _H	B _L	S	run or reference	remarks
HS0143+0549	UM 138	01 43 51.1	+05 49 57	0.018	16.2	17.7	E	l80	
HS0148+1700		01 48 32.0	+17 00 13	0.0647	16.8		B	o7	
HS0148+2123		01 48 18.4	+21 23 51	0.0165	17.2		E	o7	
HS0153+2205		01 53 17.9	+22 05 05	0.0664	18.0		E	o7	
HS0731+6348	KUG 0746+616	07 31 42.3	+63 48 27	0.3447	18.6		B	o2	Sy1
HS0732+6503		07 32 09.2	+65 03 38	0.0217	17.2		B	o1	
HS0737+6442		07 37 35.2	+64 42 18	0.036	17.7		E	l80	
HS0746+6139		07 46 54.6	+61 39 40	0.023	18.7		E	l80	
HS0747+6456		07 47 05.1	+64 56 42	0.0247	16.5		E	o2	
HS0749+5649		07 49 37.7	+56 49 48	0.0190	17.4		E	o7	
HS0750+6019		07 50 54.7	+60 19 27	0.0356	17.8		E	o2	
HS0752+5603		07 52 45.1	+56 03 07	0.0275	16.5		B	o7	
HS0752+6147		07 52 48.3	+61 47 43	0.0287	16.0		E	o1	
HS0757+6441		07 57 19.2	+64 41 52	0.0733	17.7		B	o5	
HS0805+5742		IRAS F08054+5742	08 05 25.6	+57 42 30	0.0271	17.4	B	o7	IrS
HS0808+5842		SBS 0808+587	08 08 11.0	+58 42 48	0.0272	17.7	15.5	E	l43
	VII Zw 217								IrS
	CGCG 287-051								
	CGCG 0808.1+5843								
	CGPG 0808.1+5842								
	IRAS F08082+5842								
HS0814+6439		08 14 47.8	+64 39 03	0.0390	17.1		E	o2	Sy1
HS0831+6215		08 31 18.4	+62 15 43	0.0187	17.5		E	o7	
HS0838+6253		08 38 45.2	+62 53 07	0.0044	16.0		E	o1	
HS0847+6112		MRK 0099	08 47 25.4	+61 12 30	0.0125	16.2	16.6	E	l44
	MCG +10-13-025								
	[RC2] A0847+61								
HS0912+5959	MRK 0019	09 12 54.2	+59 59 00	0.0141	16.7	16.0	E	l45	G pair, IrS
	CGCG 288-028								
	CGCG 0912.9+5959								
	MCG +10-13-071								
	IRAS 09129+5958								
	IRAS F09129+5958								
	[RC2] A0912+59								
HS0915+5540		09 15 35.8	+55 40 35	0.0494	17.2		E	o7	
HS0930+5527	MRK 0116	09 30 30.3	+55 27 46	0.0031	16.2	15.6	E	l45	
	I Zw 018								
	CGPG 0930.5+5527								
	[RC2] A0930+55B								
HS1222+3741	CG 1022	12 22 08.2	+37 41 13	0.0409	18.1		E	o7	
HS1223+3938	NPM1G +39.0289	12 23 29.8	+39 38 30	0.0360	16.8	16.92	E	o7	
HS1232+3846		12 32 15.5	+38 46 56	0.0528	17.2		E	o7	
HS1232+3947		12 32 54.6	+39 47 37	0.0210	17.2		E	o7	
HS1232+3612	KUG 1232+362	12 32 59.5	+36 12 52	0.0425	16.2		E	o7	G pair
	CG 1033								
HS1236+3821	UGC 07816	12 36 31.8	+38 21 51	0.0073	15.4		E	o7	
	CGCG 188-012								
	CGCG 1236.5+3822								
	NPM1G +38.0259								
HS1244+3648		12 44 37.0	+36 48 05	0.0472	16.4		E	o7	

Table 4: Continued

(1)	(2)	(3)	(4)	(5)	(6)	(7)	(8)	(9)	(10)
object name	other names	R.A.	Decl.	redshift	B_H	B_L	S	run or reference	remarks
HS1254+3323		12 54 46.3	+33 23 27	0.0032	17.7		B	o1	abs
HS1255+3506		12 55 22.2	+35 06 32	0.0155	17.1		E	o2	
HS1256+3505	CG 1058	12 56 02.9	+35 05 10	0.0342	16.5		E	o2	
HS1256+3512		12 56 51.2	+35 12 19	0.0035	16.8		E	o2	
HS1301+3312		13 01 05.5	+33 12 27	0.0371	17.8		E	o3	
HS1301+3325		13 01 20.0	+33 25 37	0.0246	17.5		B	o2	
HS1301+3209		13 01 59.4	+32 09 02	0.0238	17.8		E	o7	
HS1302+3046		13 02 35.4	+30 46 30	0.0355	16.0		E	o3	*
HS1304+3529	CG 1085	13 04 03.7	+35 29 43	0.0165	16.6		E	o3	
HS1306+3525	CG 1090	13 06 10.0	+35 25 40	0.0165	16.6		E	o3	
HS1306+3320		13 06 12.8	+33 20 39	0.0270	16.6		E	o3	
HS1306+3527		13 06 29.5	+35 27 25	0.0371	17.0		E	o7	
HS1308+3044	CG 0984	13 08 42.5	+30 44 55	0.0209	16.3		B	o7	
HS1309+3409	CG 1099	13 09 00.0	+34 09 11	0.0785	17.0		B	o7	
HS1309+3431	KUG 1309+345B	13 09 45.4	+34 31 15	0.0168	16.2		E	o3	spiral
HS1311+3628	UGC 08303	13 11 00.0	+36 28 02	0.0031	18.0	13.48	E	o7	IrS, HII region
	DDO 166								
	CGCG 1311.0 +3628								
	MCG +06-29-061								
	IRAS F13110+3628								
	[RC2] A1310+36								
	[RC1] A1311								
	LGG 334:[G93] 004								
HS1312+3847		13 12 14.1	+38 47 53	0.0515	17.3		E	o7	
HS1312+3508		13 12 28.3	+35 08 47	0.0035	18.1		E	o3	
HS1318+3406	CG 1131	13 18 36.1	+34 06 45	0.0352	16.6		E	o3	
HS1319+3848	NGC 5107	13 19 08.3	+38 48 05	0.00316	17.4	13.81	E	l68	IrS
	MRK 1346								
	KUG 1319+387								
	CGCG 217-033								
	CGCG 1319.1+3848								
	MCG +07-28-001								
	IRAS 13191+3847								
	IRAS F13191+3848								
	LGC 334:[G93] 011								
HS1323+3211	KUG 1323+321	13 23 16.8	+32 11 23	0.0384	16.3		E	o3	*, SBa(s)
	[SMB88] 0540								
HS1323+3319	WAS 69	13 23 31.4	+33 19 28	0.0153	16.7		E	o3	
	CG 1146								
HS1323+3316	MRK 0453	13 23 40.8	33 16 16	0.0465	16.4	16.5	E	l44	IrS
	[SMB88] 0555								
	IRAS F13236+3316								
	KUG 1323+332								
	CG 1147								

(1)	(2)	(3)	(4)	(5)	(6)	(7)	(8)	(9)	(10)
object name	other names	R.A.	Decl.	redshift	B _H	B _L	S	run or reference	remarks
HS1328+3132	UGC 08602 CGCG 1328.3+3132 MCG +05-32-035 MRK 0455 VV 326a [RC2] A1328+31 CGCG 161-074 [SMB88] 0767 CGCG 161-074E KUG 1328+315	13 28 21.5	+31 32 35	0.0342	15.3	14.6	E	l14	
HS1328+3424	KUG 1328+344	13 28 44.5	+34 24 35	0.0227	16.8		B	o7	G pair
HS1329+3703		13 29 52.7	+37 03 39	0.0557	16.9		E	o7	
HS1330+3651		13 30 54.1	+36 51 54	0.0167	16.7		E	o7	
HS1331+3906	KUG 1331+391	13 31 17.7	+39 06 32	0.0643	16.4		B	o7	
HS1332+3417	MRK 0459 [RC2] A1332+34C CG 1165	13 32 54.0	+34 17 23	0.0241	15.7	17.0	E	l44	G pair
HS1333+3149		13 33 06.8	+31 49 36	0.0248	15.9		E	o3	
HS1333+3058		13 33 17.3	+30 58 25	0.0402	17.3		E	o3	
HS1334+3957		13 34 11.5	+39 57 32	0.0083	16.9		E	o7	
HS1336+3114	CGCG 1336.2+3115 CGCG 161-097 [SMB88] 1072 KUG 1336+312	13 36 12.5	+31 14 26	0.0158	15.7		B	o7	
HS1336+3650		13 36 43.8	+36 50 56	0.0202	17.1		E	o7	
HS1338+3037	CGCG 1338.9+3038 MRK 0268 CGCG1 161-119 IRAS F13389+3037 IRAS 13388+3037 KUG 1338+306B	13 38 54.0	+30 37 51	0.0410	16.2		E	l13	G pair, IrS
HS1339+3046	MRK 0067 UGCA 372 [RC2] A1339+30 IRAS F13396+3046 KUG 1339+307	13 39 39.5	+30 46 17	0.0029	15.7	16.5	E	l51	IrS
HS1340+3307	CG 1176	13 40 08.6	+33 07 19	0.0158	16.8		E	o3	
HS1340+3207		13 40 28.3	+32 07 59	0.0365	16.8		E	o3	
HS1341+3409		13 41 50.9	+34 09 50	0.0171	17.3		E	o3	
HS1344+3511	IRAS 13448+3511 IRAS F13449+3511 CG 1189 [dKM92]	13 44 54.0	+35 11 35	0.0539	16.8	16	E	l12	IrS
HS1349+4027	MRK 0462 KUG 1349+404 CGCG 218-064 CGCG 219-009 CGCG 1349.3+4027 MCG +07-29-002 [RC2] A1349+40 NPM1G +40.0336 LGG 361:[G93] 016	13 49 17.8	40 27 35	0.0079	17.0	15.38	E	l44	
HS1349+3942	NPM1G +39.0332	13 49 22.9	+39 42 03	0.0054	16.7	15.86	E	o7	

(1)	(2)	(3)	(4)	(5)	(6)	(7)	(8)	(9)	(10)
object name	other names	R.A.	Decl.	redshift	B _H	B _L	S	run or reference	remarks
HS1353+3849	MRK 0464 KUG 1353+388 H 1350+390 XRS 13505+390	13 53 45.4	+38 49 07	0.0510	16.9	16.5	E	l13	Sy 1.5, XrayS
HS1354+3634	CG 1200	13 54 27.5	+36 34 28	0.0167	17.2		B	o7	
HS1354+3635	CG 1201	13 54 29.8	+36 35 39	0.0171	16.1	15	B	o7	
HS1400+3927	CG 0330 [SP82] 02	14 00 29.8	+39 27 37	0.0045	17.2	17	E	l78	
HS1402+3657	MRK 1369 IRAS F14021+3657 CG 0340 NPM1G +36.0325	14 02 06.6	+36 57 53	0.0120	15.5	17.0	E	l44	IrS
HS1402+3650		14 02 39.2	+36 50 45	0.0347	16.3		E	o7	
HS1408+4429	CG 0368	14 08 23.6	+44 29 01	0.0338	16.9	16	B	l88	
HS1408+4201		14 08 39.7	+42 01 06	0.0939	17.9		B	o7	abs
HS1410+3627		14 10 02.1	+36 27 15	0.0338	16.9		E	o7	
HS1410+3446	MRK 0467 [RC2] A1410+34 IRAS F14103+3447 KUG 1410+347 CG 0374	14 10 21.5	+34 46 57	0.0316	15.8	16.5	E	l44	IrS
HS1413+4402	IRAS F14131+4402	14 13 08.2	+44 02 07	0.0698	17.4		B	o7	IrS
HS1413+3956	KUG 1413+399 IRAS F14131+3955 NPM1G +39.0344	14 13 10.4	+39 56 08	0.0426	16.1	16.5	E	l6	IrS
HS1415+4203		14 15 57.1	+42 03 05	0.0683	18.1		B	o7	
HS1416+3554	KUG 1416+359	14 16 03.3	+35 54 27	0.0103	17.0	16	E	o7	spiral
HS1419+3639	UGC 09198	14 19 16.2	+36 39 19	0.0114	16.2	16.5	E	l59	Sb
HS1420+3437		14 20 59.2	+34 37 05	0.0246	18.2		E	o3	
HS1421+4018		14 21 37.9	+40 18 43	0.0982	17.6		B	o7	emi+abs
HS1422+3325		14 22 18.9	+33 25 58	0.0341	18.5		E	o3	
HS1422+3339	CG 0419	14 22 53.7	+33 39 22	0.0114	17.1		E	o3	
HS1425+3835	CG 0435	14 25 14.6	+38 35 33	0.0223	16.8	16	E	o7	
HS1429+3451	CG 0457	14 29 14.3	+34 51 17	0.0144	17.5	17.3	E	o3	
HS1429+3154	CG 1236 NPM1G +31.0320	14 29 35.4	+31 54 39	0.0117	16.7	16.9	E	o7	
HS1429+4511		14 29 45.9	+45 11 41	0.0321	18.0		E	o7	
HS1435+4523		14 35 06.7	+45 23 03	0.1267	18.3		B	o7	
HS1437+3701	MRK 0475 CG 0493	14 37 03.6	+37 01 12	0.0018	16.4	14.47	E	l44	
HS1438+3147	CG 1250	14 38 33.7	+31 47 39	0.0443	18.4	18	E	o7	
HS1440+3805	NPM1G +38.0321	14 40 08.8	+38 05 06	0.0322	16.7	17.00	B	o7	
HS1440+4302	CG 0903 NPM1G +43.0283	14 40 22.3	+43 02 32	0.0085	17.6	17.00	E	o7	
HS1442+4250		14 42 17.9	+42 50 13	0.0025	17.7		E	o7	
HS1442+4332	CG 0523	14 42 26.5	+43 32 19	0.0811	17.5	16	B	o7	**
HS1444+3114	IRAS F14440+3114 CG 1260	14 44 01.6	+31 14 23	0.0297	16.1	17	E	o7	IrS
HS1450+3844	CG 0565 [SP82] 25	14 50 21.9	+38 44 34	0.0140	17.8	16	E	l78	
HS1502+4152		15 02 31.3	+41 52 35	0.0164			B	o7	

(1)	(2)	(3)	(4)	(5)	(6)	(7)	(8)	(9)	(10)
object name	other names	R.A.	Decl.	redshift	B _H	B _L	S	run or reference	remarks
HS1504+3922	CG 0624 [SP82] 31	15 04 15.5	39 22 15	0.0302	18.8	17	E	l78	
HS1505+3944	CG 0632	15 05 53.6	+39 44 19	0.0366	17.6	16	E	o7	
HS1507+3743	CG 0644	15 07 38.1	+37 43 06	0.0322	18.3	18	E	o7	
HS1522+4214	CG 0702 NPM1G +42.0413	15 22 23.3	+42 14 40	0.0190	17.1		B	o7	
HS1524+4205		15 24 08.0	+42 05 01	0.0225	18.4		E	o7	
HS1526+4045		15 26 56.7	+40 45 17	0.0288	17.7		B	o7	
HS1543+4525		15 43 23.3	+45 25 45	0.0389	17.4		E	o3	
HS1544+4736		15 44 28.0	+47 36 20	0.0195	18.0		E	o3	
HS1546+4755		15 46 56.3	+47 55 34	0.0377	18.9		E	o3	
HS1548+4745	PC 1548+4745	15 48 04.2	+47 45 09	0.070	18.9		B	l67	
HS1549+4630	PC 1549+4630	15 49 35.5	+46 30 37	0.098	18.9		B	l67	
HS1609+4827		16 09 44.4	+48 27 44	0.0096	16.4		E	o3	
HS1610+4539		16 10 40.9	+45 39 37	0.0196	17.7		E	o3	
HS1614+4709		16 14 54.2	+47 09 22	0.0026	16.9		E	o3	
HS1626+5153	MRK 1498 IRAS F16268+5152 IRAS 16268+5152 [dKM92] 408	16 26 48.4	+51 53 05	0.0547	16.8	17.0	E	l12	Sy 1, IrS
HS1627+5239		16 27 33.1	+52 39 36	0.0288	18.3		E	o3	
HS1633+4703		16 33 12.7	+47 03 44	0.0086	16.7		E	o3	
HS1634+5218	CGCG 1634.0+5220 MRK 1499 UGC A 412 CGCG 276-029 [RC2] A1634+52 IRAS F16340+5219 CGPG 1634.0+5220 I Zw 159	16 34 07.7	+52 18 56	0.0087	15.0	16.0	E	l44	G pair, IrS
HS1640+5136	CGCG 1640.8+5138 MRK 1500 CGCG 276-037 IRAS F16408+5136 IRAS 16407+5136	16 40 48.2	+51 36 30	0.0308	15.8	15.6	E	o3	IrS
HS1641+5053	IRAS F16415+5053	16 41 31.6	+50 53 22	0.0292	16.4		E	o3	IrS
HS1643+5313		16 43 10.2	+53 13 16	0.785	19.5		E	o3	QSO
HS1645+5155		16 45 19.8	+51 55 42	0.0286	19.5		E	o3	
HS1657+5033	CGCG 1657.3+5034 CGCG 252-012 IRAS F16573+5034	16 57 22.2	+50 33 53	0.0102	16.0		E	o3	IrS
HS1657+5735	MRK 0891 IRAS F16576+5735 IRAS 16576+5735 CGPG 1657.6+5736 Zw 670	16 57 36.2	+57 35 48	0.0505	16.2		E	o3	IrS
HS1711+5758		17 11 38.2	+57 58 34	2.996	19.0		E	o7	QSO
HS1723+5631	IRAS F17237+5631	17 23 43.5	+56 31 14	0.0286	17.0		E	o3	IrS
HS1728+5655		17 28 14.4	+56 55 36	0.0160	17.0		E	o3	
HS1734+5704	IRAS F17341+5704	17 34 10.1	+57 04 58	0.0475	16.3		E	o3	IrS
HS2353+2005		23 53 39.4	+20 05 13	0.0236	17.5		E	o4	

* - galaxies with only one line detection

** - galaxies with only one line detection but twice observed

List of Abbreviations

abbrev.		reference
A	Abell galaxy	1
CG	Case Galaxy	53-57, 62-65, 71
CGCG	Catalogue of Galaxies and of Cluster of Galaxies 1968	93
CGPG	Catalogue of Selected Compact Galaxies and of Post Eruptive Galaxies 1971	92
DDO	David Dunlap Observatory catalog, van den Bergh 1966	3
[dKM92]	de Grijp, Keel, Miley et. al. 1992	12
[G93]	Garcia '93	11
H	Hard X-Ray Sources	42
IRAS	Infrared Astronomical Satellite Catalogs 1988. The Point Source Catalog	15
IRAS F	Infrared Astronomical Satellite Catalogs 1990. The Faint Source Catalog	46
KUG	Kiso Survey for UV Excess Galaxies	73-76
LGG	Lyon Group of Galaxies Catalog	11
MCG	Morphological Catalogue of Galaxies 1962	82-86
MRK	Markarian Galaxy	25-40
NPM	Lick Northern Proper Motion Program	16
OA-OZ	Ohio Source Catalog, 1415 MHz	17, 47, 18, 66, 7, 10, 8, 5, 9, 60
PC	Palomar Transit Grism Survey	67
[RC2]	The Second Reference Catalogue 1976	79
[SMB88]	Slezak, Mars, Bijaoi et. al. 1988	69
SBS	Second Byurakan Spectral Sky Survey	41, 70
[SP82]	Sanduleak and Pesch 1982	61
UCM	Universidad Complutense de Madrid	58, 89, 90
UGC	Uppsala General Catalogue of Galaxies 1973	48
UM	University of Michigan	20-24
VV	Vorontsov-Velyaminov 1959, 1977, Atlas and Catalog of Interacting Galaxies	81
WAS	Wasilewski 1983	87
XRS	Second Catalogue of X-ray Sources	2
Zw	Zwicky Compact Galaxy	91

-
1. Abell, G.O., Corwin, H.G., and Olowin, R.P. 1989, *ApJS* 70, 1
 2. Amnuel, P.R., Guseinov, O.H., and Rakhamimov, Sh. Yu. 1982, *Astrophys. and Space Sci.* 82, 3
 3. van den Bergh, S. 1966, *AJ* 71, 922
 4. Bothun, G.D., Halpern, J.P., Lonsdale, C.J., Impey, C., and Schmitz, M. 1989, *ApJS* 70, 271
 5. Brundage, R.K., Dixon, R.S., Ehman, J.R., and Kraus, J.D. 1971, *AJ* 76, 777
 6. Dey, A., and Strauss, A. 1990, *AJ* 99, 463
 7. Dixon, R.S., and Kraus, J.D. 1968, *A.J.* 73, 381
 8. Ehman, J.R., Dixon, R.S., and Kraus, J.D. 1970, *AJ* 75, 351
 9. Ehman, J.R., Dixon, R.S., Ramakrishna, C.M., and Kraus, J.D. 1974, *AJ* 79, 144
 10. Fitch, L.T., Dixon, R.S., and Kraus, J.D. 1969, *AJ* 74, 612
 11. Garcia, A.M. 1993, *A&AS* 100, 46
 12. de Grijp, M.H.K., Keel, W.C., Miley, G.K., Goudfrooij, P., and Lub, J. 1992, *A&AS* 96, 389
 13. Hewitt, A., and Burbidge, G. 1991, *ApJS* 75, 297
 14. Huchra, J.P., Geller, M.J., de Lapparent, V., and Corwin JR, H.G. 1990, *ApJS* 72, 433
 15. Joint IRAS Science Working Group 1988, *Infrared Astronomical Satellite Catalogs*, 1988, *The Point Source Catalog*, Version2.0, NASA RP-1190
 16. Klemola, A.R., Jones, B.F., and Hanson, R.B. 1987, *AJ* 94, 501
 17. Kraus, J.D. 1964, *Nature* 202, 269
 18. Kraus, J.D., Dixon, R.S., and Fisher, R.O. 1966, *Ap.J.* 144, 559
 19. Lu, N.Y., Hoffman, G.L., Groff, T., Ross, T., and Lamphier, C. 1993, *ApJS* 88, 383
 20. MacAlpine, G.M., Smith, S.B., and Lewis, D.W. 1977, *ApJS* 34, 95 (List I)
 21. MacAlpine, G.M., Smith, S.B., and Lewis, D.W. 1977, *ApJS*, 35, 197 (List II))
 22. MacAlpine, G.M., Lewis, D.W., Smith, S.B. 1977, *ApJS* 35, 203 (List III)
 23. MacAlpine, G.M., Lewis, D.W. 1978, *ApJS* 36, 587 (List IV)
 24. MacAlpine, G.M., and Williams, G.A. 1981, *ApJS* 45, 1113 (List V)
 25. Markarian, B.E., 1967, *Astrofizika* 3, 55
 26. Markarian, B.E., 1969, *Astrofizika* 5, 443
 27. Markarian, B.E., and Lipovetskii, V.A. 1969, *Astrofizika* 5, 581
 28. Markarian, B.E., and Lipovetskii, V.A. 1971, *Astrofizika* 7, 511
 29. Markarian, B.E., and Lipovetskii, V.A. 1972, *Astrofizika* 58, 155
 30. Markarian, B.E., and Lipovetskii, V.A. 1973, *Astrofizika* 9, 487
 31. Markarian, B.E., and Lipovetskii, V.A. 1974, *Astrofizika* 10, 307
 32. Markarian, B.E., and Lipovetskii, V.A. 1976a, *Astrofizika* 12, 389
 33. Markarian, B.E., and Lipovetskii, V.A. 1976b, *Astrofizika* 12, 657
 34. Markarian, B.E., Lipovetskii, V.A., and Stepanian, D.A. 1977a, *Astrofizika* 13, 225
 35. Markarian, B.E. Lipovetskii, V.A., and Stepanian, D.A. 1977b, *Astrofizika* 13, 397
 36. Markarian, B.E. Lipovetskii, V.A., and Stepanian, D.A. 1979a, *Astrofizika* 15, 201
 37. Markarian, B.E. Lipovetskii, V.A., and Stepanian, D.A. 1979b, *Astrofizika* 15, 363
 38. Markarian, B.E. Lipovetskii, V.A., and Stepanian, D.A. 1979c, *Astrofizika* 15, 54
 39. Markarian, B.E. Lipovetskii, V.A., and Stepanian, D.A. 1981, *Astrofizika* 17, 61
 40. Markarian, B.E., Lipovetskii, V.A., and Stepanian, D.A. 1983, *Astrofizika* 19, 221
 41. Markarian, B.E., and Stepanian, J.A. 1983, *Astrophysics* 19, 354; *Astrofizika* 19, 639
 42. Marshall, F.E., Boldt, E.A., Holt, S.S., Mushotzky, R.F., Pravdo, S.H., Rothschild, R.E., and Serlemitsos, P.J. 1979, *ApJS* 40, 657
 43. Martel, A., and Osterbrock, D.E. 1994, *AJ* 107, 1283
 44. Mazzarella, J.M., and Balzano, V.A. 1986, *ApJS* 62, 751
 45. Mazzarella, J.M., and Boroson, T.A. 1993, *ApJS* 85, 27
 46. Moshir, M., Kopan, G., Conrow, T., Mccallan, H., Hacking, P., Gregorich, D., Rohrbach, G., Melnyk, M., Rice, W. Fullmer, L., et. al. 1990, *Infrared Astronomical Satellite Catalogs*, 1990, *The Faint Source Catalog*, Version 2.0
 47. Nash, R.T. 1965, *AJ* 70, 846
 48. Nilson, P. 1973, *Uppsala General Catalogue of Galaxies*, *Nova Acta Regiae Societatis Scientiarum Ser. V*, Vol.1, Uppsala
 49. Noguchi, T., Maehara, H., and Kondo, M. 1980, *Ann. Tokio Astron. Obs.*, 2-nd Series 18, 55
 50. Osterbrock, D.E., and Pogge, R.W. 1987, *ApJ* 323, 108
 51. Osterbrock, D.E., and Shaw, R.A. 1988, *ApJ* 327, 89
 52. Palumbo, G.C.G., Tanzella-Nitti, G., and Vettolani, G. 1983, *Catalog of Radial Velocities of Galaxies*, New-York: Gordon&Breach
 53. Pesch, P., Sanduleak, N. (Paper I) 1983, *ApJS* 51, 171
 54. Pesch, P., Sanduleak, N. (Paper III) 1986, *ApJS* 60, 543
 55. Pesch, P., Sanduleak, N. (Paper V) 1988, *ApJS* 66, 297
 56. Pesch, P., Sanduleak, N. (Paper VIII) 1989, *ApJS* 70, 163
 57. Pesch, P., Sanduleak, N., and Stephenson, C.B. (Paper XII) 1991, *ApJS* 76, 1043
 58. Rego, M., Cordero-Gracia, M., Zamorano, J. and Gallego, J. 1993, *AJ* 105, 427
 59. Richter, O.-G., and Huchtmeier, W.K. 1991, *A&AS* 87, 425
 60. Rinsland, C.P., Dixon, R.S., Gerhart, M.R., and Kraus, J.D. 1974, *AJ* 79, 1129
 61. Sanduleak, N. and Pesch, P. 1982, *ApJ* 258, L11
 62. Sanduleak, N., Pesch, P. (Paper II) 1984, *ApJS* 55, 517
 63. Sanduleak, N., and Pesch, P. (Paper IV) 1987, *ApJS* 63, 809
 64. Sanduleak, N., Pesch, P. (Paper IX) 1989, *ApJS* 70, 173
-

References to the Table 4. Continued

65. Sanduleak, N., Pesch, P. (Paper XI) 1990, ApJS 72, 291
66. Scheer, D.J., and Kraus, J.D. 1967, A.J. 72, 536
67. Schneider, D.P., Schmidt, M., and Gunn, J.E., 1994, AJ 107, 1245
68. Schneider, S.E., Thuan, T.X., Mangum, J.G. and Miller, J. 1992, ApJS 81, 5
69. Slezak, E., Mars, G., Bijaoui, A., Balkowski, C., and Fontanelli, P. 1988, A&AS 74, 83
70. Stepanian, J.A., Lipovetski, V.A. and Erastova, L.K. 1990, Astrophysics 32, 252; Astrofizika 32, 441
71. Stephenson, C.B., Pesch, P., and MacConnell, D.J. (Paper XIII) 1992, ApJS 82, 471
72. Strauss, M.A., Huchra, J.P., Davis, M., Yahil, A., Fisher, K.B., and Tonry, J. 1992, ApJS 83, 29
73. Takase, B., and Miyauchi-Isobe, N. 1984, Annals of the Tokio Ast. Obs. 19, 595
74. Takase, B., and Miyauchi-Isobe, N. 1986, Annals of the Tokio Ast. Obs. 21, 181
75. Takase, B., and Miyauchi-Isobe, N. 1987, Annals of the Tokio Ast. Obs. 21, 251
76. Takase, B., and Miyauchi-Isobe, N. 1989 Pub. National Ast. Obs. of Japan 1, 11
77. Terlevich, R., Melnick, J., Masegosa, J., Moles, M., and Copetti, M.V.F. 1991, A&AS 91, 285
78. Tift, W.C., Kirshner, R.P., Gregory, S.A., Moody, J.W. 1986, ApJ 310, 75
79. de Vaucouleurs, G., de Vaucouleurs, A., and Corwin, H.G. 1976, Second Reference Catalogue of Bright Galaxies, University of Texas Press, Austin
80. Vogel, S., Engels, D., Hagen, H.-J., Groote, D., Wisotzki, L., Cordis, L., and Reimers, D. 1993, A&AS 98, 193
81. Vorontsov-Velyaminov, B.A. 1959, Atlas and Catalog of Interacting Galaxies, Sternberg. Inst., Moscow State University
82. Vorontsov-Velyaminov, B.A., and Krasnogorskaja, A.A. 1962, Morphological Catalog of Galaxies, Part I Moscow State University
83. Vorontsov-Velyaminov, B.A., and Arhipova, V.P. 1964, Morphological Catalog of Galaxies, Part II Moscow State University
84. Vorontsov-Velyaminov, B.A., and Arhipova, V.P. 1963, Morphological Catalog of Galaxies, Part III Moscow State University
85. Vorontsov-Velyaminov, B.A., and Arhipova, V.P. 1968, Morphological Catalog of Galaxies, Part IV Moscow State University
86. Vorontsov-Velyaminov, B.A., and Arhipova, V.P. 1974, Morphological Catalog of Galaxies, Part V Moscow State University
87. Wasilewski, A.J. 1983, ApJ 272, 68
88. Weistrop, D., and Downes, R.A. 1988, ApJ 331, 172
89. Zamorano, J., Rego, M., Gonz  les-Riestra, R. 1989, 79, 443
90. Zamorano, J., Rego, M., Gallego, J., Vitores, A.G., Gonz  les-Riestra, R., and Rodr  guez-Caderot, G.
91. Zwicky, F. 1961-1968, Seven privately circulated lists.
92. Zwicky, F. 1971, Catalogue of Selected Compact Galaxies and of Post Eruptive Galaxies
93. Zwicky, F., Herzog, E., Wild, P., Karpowicz, M., and Kowal, C. 1961-1968, Catalog of Galaxies and of Clusters of Galaxies, Pasadena: California Institute of Technology

Complete follow-up spectroscopy of our first-priority candidates was accomplished. With a success rate of detecting true emission-line objects of 76%, this provides the bulk of our sample of ELGs. As mentioned in § 2, we also observed 83 second priority candidates, in order to test their nature. From these, many were stars, but we also found 23 emission line galaxies, one galaxy with emission and absorption, four galaxies with absorption lines and a QSO. The efficiency of finding emission line objects in the second priority sample is then 28%. This result is biased, because we observed mostly candidates that showed extended images on the direct plates. From the 23 emission line galaxies we found, 21 had obvious extended images, and only two looked like point sources. If one takes random candidates from the second priority list, the efficiency is as low as 10%. From the 23 galaxies with emission, only two had intermediate ionization spectra that could be detected in the IIIa-J objective plates. The others showed either low or very low ionization spectra, with faint H_β and [OIII], or spectra with only H_α , or H_α and [SII]. These objects cannot be seen as emission-line candidates in the IIIa-J objective plate. We conclude then that there is no way to distinguish real emission-line galaxies from the rest of non-emission blue candidates. Taking into account the low efficiency of finding emission-line objects, such a blind search would cost too much telescope time. We believe that such objects can be very easily recognised in an IIIa-F survey (like that of Zamorano et al. 1994). Therefore, we do not intend to complete the follow-up spectroscopy for the second priority objects, and we leave them to the discovery of the $H\alpha$ surveys.

We obtained a final sample of 203 objects, of which 196 are emission-line galaxies, four are galaxies with absorption, and three are QSOs. From our sample of 203 objects, 98 (48%) are newly discovered objects, 52 (26%) are objects found already in the literature but with no available redshift (sometimes mentioned only as IRAS sources or only as NPM (Lick Northern Proper Motion Program) galaxies) and 53 (26%) are objects with redshifts given already in the literature. We have observed all the objects with unknown redshift. From the objects with available redshifts, five were reobserved, in order to estimate our redshift errors (see Section 3). The mean surface density of the emission-line galaxies of our survey is 0.16 deg^{-2} . This number is quite low in comparison with the mean surface density of 0.46, found by Salzer et al. (1989). But one must keep in mind that this is a sample of candidates selected in a special parameter region. We select our candidates in a certain “brightness” range and in a certain “colour” range. We are also losing the low-ionization galaxies into the second category objects, as discussed above. Thus our sample is dominated by high ionization galaxies, which should not come as a surprise, since the final selection was on the [OIII] line strengths.

The apparent magnitudes (derived from the Hamburg prism plates) of our sample range between $15.0 \leq B \leq 19.5$. We have selected all available magnitudes (56) from the literature for our sample (Table 4) and compare this heterogeneous data set with our own magnitude estimates (Fig. 5). The values agree sufficiently well below 16 mag, if we assume internal errors of about 0.5 mag in each sample. For the literature values, 0.5 mag is an estimated mean error, as these data came from various sources, with different measurement methods and calibrations. The estimated error for the prism plate magnitudes is known to be 0.5 mag. For galaxies with

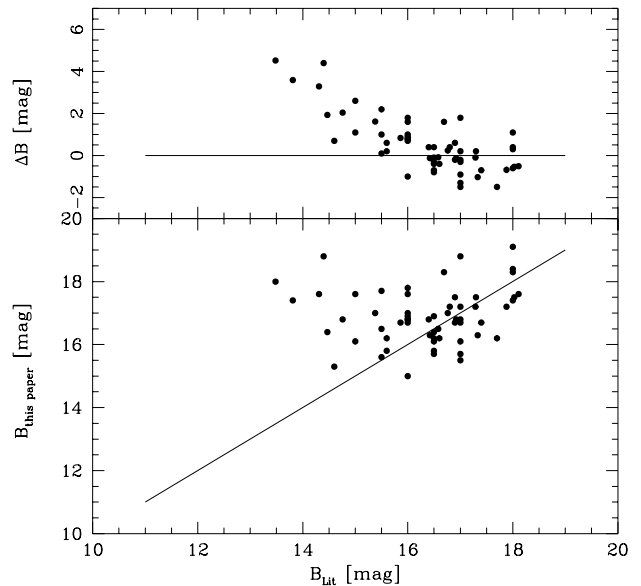


Fig. 5. The comparison between our Hamburg objective prism magnitudes B_H and the magnitudes from literature, B_L . In the bottom panel we plotted B_H versus B_L . The solid line represents $B_H = B_L$. In the top panel we plotted the difference $\Delta B = B_H - B_L$ versus B_L .

$B \leq 16$, our magnitudes seem to underestimate the total flux of the galaxies systematically. This can easily be explained by the fact that the objective prism spectra show up only with the bright HII region (or the core of the galaxy), while the fainter surrounding, without emission lines, is not detectable on these plates (see remarks in Table 4). A typical example is HS0108+0103, an Sdm galaxy, that we see only as an HII knot. The apparent magnitude of 17.6 describes only the flux that comes from the HII region, as compared with the value of 14.31^m of the whole galaxy. Another example is HS0137+1539, a very compact source near the edge of the low-surface brightness Im galaxy, DDO 013. With $B=18.8$, as compared with the $B=14.4$ apparent magnitude of the DDO, it was not obvious if the candidate was a separate object, or part of the DDO galaxy. A long slit spectra of the object confirmed that it belongs to the DDO galaxy. The same situation happened with HS1311+3628. The galaxy was reobserved in order to see if the emission knot we found is a separate galaxy or an HII region in the DDO 166. As the redshifts agree, the source we found is an HII region (apparent magnitude 18.0 instead of 13.48). Other galaxies where we subestimate the contribution of the underlying galaxies are: HS0122+0743 ($B=17.6$ instead of $B=15.00$), HS0808+5842 ($B=17.7$ instead of $B=15.5$), HS1332+3417 ($B=15.7$ instead of $B=17.0$), HS1349+4027 ($B=17.0$ instead of 15.38), HS1437+3701 ($B=16.4$ instead of $B=14.47$).

To have a further independent comparison of our magnitudes, we used the on-line facility of the APM catalogue as

Table 5: The emission-lines detected in the spectra of the observed objects

object name	emission lines
HS0000+2252	[OII], H δ , H γ , H β , [OIII], [OIII], HeI, H α + [NII], HeI, [SII]
HS0000+2422	[OII], H β , [OIII], [OIII], H α , [SII]
HS0013+0809	[OIII], H α
HS0013+1942	Mgb, NaI, H α
HS0013+2241	[OII], H β , [OIII], [OIII], [OI]?, H α + [NII], [SII]
HS0016+1449	[OII], H β , [OIII], [OIII], H α , [SII]
HS0021+1347	[OII], H β , [OIII], [OIII], H α , [SII],
HS0022+0014	[OII], H β , [OIII], [OIII], HeI, H α + [NII], [SII]
HS0024+1022	[OII], H β , [OIII], [OIII], H α , [SII],
HS0022+1945	H α , [SII]
HS0024+2314	[OII], H β , [OIII], [OIII], H α , [SII]
HS0026+0332	[OII], H β , [OIII], [OIII], HeI?, H α , [SII]
HS0028+1747	H β , H α
HS0029+1748	[NeIII], H ζ , H ϵ , H δ , H γ , [OIII], H β , [OIII], [OIII], HeI, H α + [NII], HeI, [SII], [AIII], [OII]
HS0029+1443	[OII], [NeIII], H ζ , H ϵ , H δ , H γ , [OIII], H β , [OIII], [OIII], HeI, [OI] H α + [NII], HeI, [SII], [AIII], [OII], [AIII]
HS0035+0725	QSO: MgII
HS0036+0437	[OII], H β , [OIII], [OIII], H α , [SII]
HS0036+0352	[OII] ?
HS0037+0111	[OII], H β , [OIII], [OIII], H α + [NII], [SII]
HS0040+0952	[OII], H γ , H β , [OIII], [OIII], [OI]?, H α , [SII]
HS0041+2333	[OII], [NeIII], H ζ , [NeIII]+[OII]+H ϵ ?, H δ , H γ , H β , [OIII], [OIII], HeI, H α , HeI?, [SII]
HS0043+0531	[OII], H β , [OIII], [OIII], H α + [NII], [SII]
HS0045+0020	H β , [OIII], [OIII], H α , [SII]
HS0051+0927	H β , [OIII], [OIII], HeI, H α + [NII], [SII]
HS0052+2119	[OII], H β , [OIII], [OIII], HeI?, H α , [SII]
HS0056+0044	[OII], H β , [OIII], [OIII], H α , [SII]
HS0058+1847	[OII], [NeIII], H ϵ , H δ , H γ , H β , [OIII], [OIII], HeI, [OI], H α + [NII], [SII], [AIII]
HS0101+0310	[OII], [NeIII]?, H γ ?, H β , [OIII], [OIII], HeI?, H α , [SII]
HS0103+2441	[OII], H β , [OIII], [OIII], H α , [SII]
HS0103+1242	[OII], H γ ?, H β , [OIII], [OIII], HeI?, H α + [NII], [SII]
HS0106+1304	[OII], [NeIII], H β , [OIII], [OIII], [OI], H α + [NII], [SII]
HS0107+1946	H β , [OIII], H α + [NII], [SII]
HS0107+2458	[OII], H β , [OIII], [OIII], H α , [SII]
HS0108+0150	H β , [OIII], [OIII], H α , [SII]
HS0110+2149	H β , [OIII], [OIII], H α + [NII], [SII]
HS0111+2115	[OII], [NeIII], H ζ , H ϵ , H δ , H γ , H β , [OIII], [OIII], HeI, [OI], H α , [SII], [AIII]
HS0113+1750	[OII], [NeIII], H ζ , H ϵ , H δ , H γ , [OIII], H β , [OIII], [OIII], HeI, [OI], H α , HeI, [SII], [AIII]
HS0116+2244	abs: H β , Mgb, NaD
HS0117+1017	[OII], H γ , [OIII], [OIII]
HS0117+1135	[NII]+H α + [NII], [SII]
HS0118+1236	[OII], H γ , [OIII], [OIII]
HS0119+0331	[OII], H β , [OIII], [OIII], HeI?, [OI]?, H α + [NII], [SII]
HS0123+1624	H γ , H β , [OIII], [OIII], HeI, [OI], H α , [SII]
HS0124+1126	[OII], [OIII], [OIII]
HS0131+1937	H β , [OIII], [OIII], H α + [NII], [SII]
HS0133+1341	H β , [OIII], [OIII], H α + [NII], [SII]
HS0137+1539	H β , [OIII], [OIII], H α + [NII], [SII]
HS0143+2400	[OII], [NeIII], H ζ , H ϵ , H δ , H γ , [OIII], H β , [OIII], [OIII], HeI, H α , HeI, [SII], [AIII]
HS0148+1700	[OII], H γ , H β , [OIII], [OIII], [OI], H α + [NII], [SII]

object name	emission lines
HS0148+2123	H δ , H γ , H β , [OIII], [OIII], HeI, H α + [NII], [SII], [AIII]
HS0153+2205	[OIII], [NII]+H α + [NII], [SII]
HS0731+6348	Sy1: MgII, H γ , H β , [OIII], [OIII], H α
HS0732+6503	H α + [NII], [SII]
HS0747+6456	[OII], [NeIII], H β , [OIII], [OIII], [OI], H α , [SII],
HS0749+5649	[NeIII], H ζ , H ϵ , H δ , H γ , [OIII], H β , [OIII], [OIII], HeI, [OI], H α + [NII], HeI, [SII], [AIII]
HS0750+6019	[OII], [NeIII], H β , [OIII], [OIII], H α , [SII],
HS0752+5603	H γ , H β , [OIII], [OIII], HeI, [OI], H α + [NII], [SII], [AIII]
HS0752+6147	[OII], H γ , H β , [OIII], [OIII], HeI
HS0757+6441	[OII], H β , [OIII], [OIII], H α , [SII]
HS0805+5742	H γ , H β , [OIII], [OIII], HeI, [OI], H α + [NII], [SII]
HS0814+6439	Sy1: [OII], H δ , H γ , H β , [OIII], [OIII], H α , [SII],
HS0831+6215	[NeIII], H δ , H γ , [OIII], H β , [OIII], [OIII], HeI, [OI], H α + [NII], HeI, [SII], [AIII]
HS0838+6253	[OII], H γ , H β , [OIII], [OIII] -incomplete spectrum
HS0915+5540	[NeIII], H δ , H γ , [OIII], H β , [OIII], [OIII], HeI, HeI, [OI], [OI], H α + [NII], [SII], [AIII]
HS1222+3741	[OII], [NeIII], H γ , H β , [OIII], [OIII], HeI, H α , [SII]
HS1223+3938	[OII], H β , [OIII], [OIII], H α + [NII], [SII]
HS1232+3846	[OII], H β , [OIII], [OIII], H α + [NII], [SII]
HS1232+3947	[NeIII], H δ , H γ , H β , [OIII], [OIII], HeI, H α , [SII]
HS1232+3612	[OII], [NeIII], H γ , H β , [OIII], [OIII], HeI, [OI], H α + [NII], [SII], [AIII]
HS1236+3821	H β , [OIII], [OIII], H α + [NII], [SII]
HS1244+3648	[OII], H β , [OIII], [OIII], H α + [NII], [SII]
HS1254+3323	abs: CaK, G $_{band}$, NaD, Mgb?
HS1255+3506	[OII], H β , [OIII], [OIII], H α , [SII],
HS1256+3505	[OII], H β , [OIII], [OIII], H α , [SII],
HS1256+3512	[OII], H β , [OIII], [OIII], H α , [SII],
HS1301+3312	H β , [OIII], [OIII], H α , [SII]
HS1301+3325	[OII], H β , [OIII], [OIII], H α
HS1301+3209	H β , [OIII], [OIII], H α + [NII], [SII] [AIII], [OII]
HS1302+3046	H α
HS1304+3529	H γ , H β , [OIII], [OIII], H α + [NII], [SII]
HS1306+3525	[OIII], H α
HS1306+3320	H β , [OIII], [OIII], H α , [SII]
HS1306+3527	H α , [SII]
HS1308+3044	H β , [OIII], [OIII], H α + [NII], [SII]
HS1309+3409	H β , H α
HS1309+3431	[OIII], H α + [NII], [SII]
HS1311+3628	[NeIII], H ζ , H ϵ , H δ , H γ , [OIII], H β , [OIII], [OIII], HeI, [OI], [OI], H α , HeI, [SII], [AIII], [OII]
HS1312+3847	[OII], [NeIII], H ζ , H ϵ , H δ , H γ , H β , [OIII], [OIII], HeI, [OI], H α , [SII], [AIII]
HS1312+3508	H γ , H β , [OIII], [OIII], HeI, [OI]+ [SII], [OI], H α HeI, [SII], HeI, [AIII], [OII], [AIII]
HS1318+3406	H β , [OIII], [OIII], H α , [SII]
HS1323+3211	H α
HS1323+3319	H γ , H β , [OIII], [OIII], HeI, [OI], H α , [SII]
HS1328+3424	H β , [OIII], [OIII], H α + [NII], [SII]
HS1329+3703	[OII], H β , [OIII], [OIII], H α + [NII], [SII]
HS1330+3651	[NeIII], H ϵ , H δ , H γ , H β , [OIII], [OIII], HeI, [OI], H α + [NII], [SII], [AIII]
HS1331+3906	H α + [NII], [SII]
HS1333+3149	[OIII], H α + [NII]

object name	emission lines
HS1333+3058	H γ , H β , [OIII], [OIII], HeI, H α , [SII]
HS1334+3957	[NeIII], H ϵ , H δ , H γ , [OIII], H β , [OIII], [OIII], HeI, H α + [NII], [SII], [AIII]
HS1336+3114	H β , [OIII], [OIII], H α + [NII], [SII]
HS1336+3650	H β , [OIII], [OIII], H α
HS1340+3307	H β , [OIII], [OIII], HeI, H α , [SII]
HS1340+3207	H β , [OIII], [OIII], H α , [SII]
HS1341+3409	H β , [OIII], [OIII], H α , [SII]
HS1349+3942	H β , [OIII], [OIII], H α + [NII], [SII]
HS1354+3634	H γ , H β , [OIII], [OIII], HeI, [OI], H α + [NII], [SII]
HS1354+3635	H β , [OIII], [OIII], H α + [NII], [SII]
HS1402+3650	[OII], H γ , H β , [OIII], [OIII], HeI, H α + [NII], [SII]
HS1408+4201	abs: Mgb, NaD
HS1410+3627	[OII], H β , [OIII], [OIII], H α , [SII]
HS1413+4402	[OII], H β , [OIII], [OIII], H α + [NII], [SII]
HS1415+4203	H α + [NII]
HS1416+3554	[NeIII], H β , [OIII], [OIII], HeI, [OI], H α + [NII], [SII]
HS1420+3437	H β , [OIII], [OIII], HeI, [OI], H α , [SII]
HS1421+4018	abs: CaH, G $band$, Mgb, NaD emi: [OII], H α + [NII]?, [SII]
HS1422+3325	H β , [OIII], [OIII], HeI, [OI], H α , [SII]
HS1422+3339	H β , [OIII], [OIII], H α , [SII]
HS1425+3835	H β , [OIII], [OIII], H α + [NII], [SII]
HS1429+3451	H γ , H β , [OIII], [OIII], HeI, [OI], H α , HeI?, [SII]
HS1429+3154	H γ , H β , [OIII], [OIII], HeI, H α , [SII]
HS1429+4511	H β , [OIII], [OIII], H α + [NII], [SII]
HS1435+4523	[OII], H β , [OIII], [OIII], H α + [NII], [SII]
HS1438+3147	[OII], [NeIII], H γ , [OIII], H β , [OIII], [OIII], HeI, [OI], H α , [SII]
HS1440+3805	H β , [OIII], [OIII], HeI, [OI], H α + [NII], [SII]
HS1440+4302	[NeIII], H γ , H β , [OIII], [OIII], HeI, [OI], H α + [NII], [SII], [AIII]
HS1442+4250	[NeIII], H ζ , H ϵ , H δ , H γ , [OIII], H β , [OIII], [OIII], HeI, [OI], H α , [SII], [AIII]
HS1442+4332	H α ?
HS1444+3114	H β , [OIII], [OIII], H α + [NII], [SII]
HS1502+4152	H β , [OIII], [OIII], H α , [SII]
HS1505+3944	H α , [SII]
HS1507+3743	[OII], [NeIII], H ζ , H ϵ , H δ , H γ , [OIII], H β , [OIII], [OIII], HeI, [OI], H α , [SII], [AIII]
HS1522+4214	H β , [OIII], [OIII], H α + [NII], [SII]
HS1524+4205	[OIII], [OIII], H α + [NII], [SII]
HS1526+4045	[OIII], H α , [SII]
HS1543+4525	H β , [OIII], [OIII], HeI, [OI], H α , [SII], [AIII] emi: [OII], [SII]
HS1544+4736	H γ , H β , [OIII], [OIII], HeI, H α , [SII], [AIII]
HS1546+4755	H β , [OIII], [OIII], H α , [SII]
HS1609+4827	H β , [OIII], [OIII], HeI?, [OI]?, H α + [NII], [SII]
HS1610+4539	H γ , H β , [OIII], [OIII], HeI, [OI], H α , [SII], [AIII]
HS1614+4709	H γ , H β , [OIII], [OIII], HeI, [OI], H α , [SII], [AIII]
HS1633+4703	H β , [OIII], [OIII], H α , [SII]
HS1640+5136	H γ ?, HeII?, H β , [OIII], [OIII], HeI, [OI], H α + [NII], [SII]
HS1641+5053	H β , [OIII], [OIII], HeI, [OI], H α + [NII], [SII]
HS1643+5313	QSO: MgII, FeII
HS1645+5155	H β , [OIII], [OIII], H α , [SII]
HS1657+5033	H β , [OIII], [OIII], HeI, [OI], H α , [SII]
HS1657+5735	H β , [OIII], [OIII], HeI, [OI], H α , [SII]
HS1627+5239	H β , [OIII], [OIII], HeI, H α , [SII]

HS1645+5155	H β , [OIII], [OIII], H α + [NII], [SII]
HS1711+5758	QSO: Ly α , [OI]?, CIV
HS1723+5631	H β , [OIII], [OIII], HeI, H α , [SII]
HS1728+5655	H γ , H β , [OIII], [OIII], [HeI], [OI]?, H α ,
HS1734+5704	H γ , H β , [OIII], [OIII], HeI, [OI], H α , [SII]
HS2353+2005	H β , [OIII], [OIII], H α + [NII], [SII]

The complete sequence of emission lines listed in the table (wavelengths given in Å): Ly α 1216, NV 1240, CIV 1549, MgII 2798, [OII] (blend) 3727.45, [NeIII] 3868.76, H ζ (blend HeI) 3889.05 (3889.65), H ϵ (blend [NeIII], [OII]) 3970.07 (3967.47, 3967.40), H δ 4101.6, H γ 4340.3, [OIII] 4363.21, HeII 4686, H β 4861.2, [OIII] 4958.92, [OIII] 5006.85, HeI 5875.99, [OI] (blend with [SII]) 6300.32 (6312.1), [OI] 6363.81, [NII] 6548.2, H α 6562.9, [NII] 6583.6, HeI 6678.1, [SII] (blend) 6723.6, HeI 7065.3, [AIII] 7135.8, [OII] (blend) 7319.9, 7330.2, [AIII] 7751.02

described by Maddox et al. (1990), Irwin, Maddox & McMahon (1994). All objects with new redshifts have been searched in the APM catalogue facility and 146 have been retrieved by comparison of their position only. It is beyond the scope of this paper to clarify why some sources were missed. We note that there is no significant deviation between the RA and δ values from our measurements and those of the APM:

$$[RA_{(this\ paper)} - RA_{APM}] = -0.04 \pm 0.11\ sec$$

$$[\delta_{(this\ paper)} - \delta_{APM}] = -0.62 \pm 1.25\ arcsec$$

and, that the error distribution corresponds to our expectations (see above). The comparison of the B magnitudes, however, shows a surprising distribution (Fig. 6). The difference between the APM magnitudes and ours seems to increase monotonically with brightness, with a scatter of about ± 1.4 mag. superimposed. For fainter ($B \geq 16$) galaxies one may understand the diagram in the sense of a small offset and a magnitude error in both samples in the order of 0.4 to 0.5 mag. The differences for the brighter objects however cannot be explained as before. According to the APM magnitudes, one would expect that we have NGC and even Shapley-Ames galaxies in our sample, which is not the case. The distribution ranges up to the unrealistic $B_{APM}=11$ mag. This may mean that there are still some uncertainties in the calibration of the APM magnitudes for the bright objects, where the plates tend to be saturated over a large extent of the galaxy (see also Metcalfe et al. 1995). We finally conclude that the subsample of our objects with $16 \leq B \leq 19.5$ have good total luminosity estimates, while for the brighter ones, our values are only lower limits. It is customary to give a magnitude for which a survey is complete, but for our sample the incompleteness are also described in terms of colour, line fluxes and equivalent widths of the emission lines. (A detailed description of the incompleteness will be given in a future paper).

If we exclude the emission-line galaxies that were found as second priority objects, we find that our objects have redshifts between $0 < z < 0.1$, which is exactly the range for which the [OIII] line and/or H β can be seen in the IIIa-J plates, due to

the cutoff of the emulsion at 5400 Å. In Fig. 7 we give the redshift distribution of our sample. With dotted line we plot the whole sample, included the blue candidates, while with solid line we plot only the first priority objects. The histogram has a peak at $z=0.015$, which shows that our sample is dominated by nearby galaxies (as intended for a study of the nearby large scale structure). The histogram drops very fast after 0.06, containing only a few objects with $0.06 < z < 0.10$, most of them being blue objects. The few galaxies with $z > 0.1$ are also from the second category objects.

5. Conclusions

Our survey for emission-line galaxies contains a complete sample based on candidates selected from digitized objective prism plates. We used the IIIa-J plates taken in the frame of the Hamburg QSO Survey. Automated search software is applied to the digitized data to select spectra in a certain parameter space. The two selection criteria are the “brightness” and the “colour” of the spectra. The selected candidates are then rescanned with high resolution and the final digitized spectra are visually inspected for emission lines. Some second priority candidates were also selected because of their blue spectra. We observed all the first priority candidates and also some of the second priority ones.

1. The final sample contains 203 objects, of which 196 are ELG, four are galaxies with absorption and three are QSOs. Almost half of our sample contains newly discovered objects, and three quarters of the given redshifts are new.

2. The mean surface density of our sample of emission-line galaxies is 0.16. This value is lower than the value obtained by the Michigan Survey, for example, but our sample is selected with an automated procedure, in a certain interval of parameters.

3. Our galaxies have apparent magnitudes between $15.0 < B < 19.5$. A comparison with the magnitudes available in the literature, as well as with the APM ones, shows that our magnitudes are reliable only for the compact faint objects. In the

Table 6: List of identified stars

object name	coord.	B	type	abs. lines
HS0007+0520	00 07 16.1 +05 20 42	19.4	M	
HS0014+0351	00 14 34.5 +03 51 43	18.0		Mgb?
HS0015+1123	00 15 18.3 +11 23 00	18.4	M	
HS0018+2040	00 18 35.1 +20 40 36	18.7	G	H β , Mgb
HS0019+0006	00 19 20.5 +00 06 30	17.4		H γ , H β , H α
HS0024+2413	00 24 55.6 +24 13 43	17.3	G	CaK, CaH, G $_{band}$, H β , Mgb, NaI, H α
HS0028+1201	00 28 31.3 +12 01 18	17.9	F or G	Mgb, NaI, H α
HS0028+2419	00 28 41.7 +24 19 50	17.8	G	G $_{band}$, Mgb, H α
HS0030+1433	00 30 17.2 +14 33 09	17.4	F	G $_{band}$, H β , Mgb, H α
HS0039+2151	00 39 53.0 +21 51 37	16.8	F	G $_{band}$, H α
HS0040+1344	00 40 28.8 +13 44 15	18.2	F or G	H β , NaD, H α
HS0103+1520	01 03 19.3 +15 20 20	17.6	late-type star	Mgb, H α
HS0107+0006	01 07 58.7 +00 06 53	17.8	G	CaK, CaH, H β , H α
HS0109+1540	01 09 30.0 +15 40 07	15.8	early-type star	H β , H α
HS0739+6019	07 39 07.4 +60 19 32	18.0	G	G $_{band}$, H β , Mgb, H α
HS0750+6337	07 50 44.4 +63 37 29	18.1	M	
HS0753+5645	07 53 41.8 +56 45 12	17.1	G	CaK, CaH, G $_{band}$, H β , H α
HS0815+5658	08 15 58.9 +56 58 19	17.4	late-type star	Mgb, NaD, H α
HS1311+3350	13 11 21.4 +33 50 01	17.7	A	CaH, H δ , H γ , H β , H α
HS1313+3127	13 13 29.9 +31 27 04	18.0		Mgb, H α
HS1315+3340	13 15 17.3 +33 40 27	18.4		H β , NaI
HS1328+3528	13 28 28.4 +35 28 39		F or G	CaK, CaH, G $_{band}$, H β , H α
HS1406+3427	14 06 42.5 +34 27 55	16.5	G	G $_{band}$, FeI, H β , Mgb, NaD, H α
HS1406+3844	14 06 22.2 +38 44 39		A or F	H δ , G $_{band}$, H γ , H β , H α
HS1416+3932	14 16 30.3 +39 32 11		F	CaK, CaH, G $_{band}$, H β , H α
HS1419+4116	14 19 29.9 +41 16 14		M	
HS1427+4200	14 27 12.9 +42 00 58		A or F	CaK, CaH, H β , H α
HS1432+4255	14 32 38.5 +42 55 30		M	
HS1445+4412	14 45 17.9 +44 12 06			H α
HS1448+3952	14 48 32.3 +39 52 39		F or G	CaK, G $_{band}$, H β , H α
HS1452+3009	14 52 25.2 +30 09 06		A	CaK, CaH, H δ , G $_{band}$, H β , H α
HS1502+3444	15 02 38.7 +34 44 55		F or G	CaK, CaH, G $_{band}$, H β , Mgb, NaD, H α
HS1503+3822	15 03 21.8 +38 22 41		A or F	CaK, CaH, H δ , H γ , H β , H α
HS1508+4025	15 08 05.2 +40 25 29		F	CaK, CaH, H δ , H γ , H β , Mgb, H α
HS1510+3551	15 10 40.6 +35 51 16		late-type star	CaK, CaH
HS1516+4441	15 16 19.1 +44 41 45		M	
HS1517+4021	15 17 55.0 +40 21 32		F or G	CaK, CaH, G $_{band}$, H β , Mgb, H α
HS1523+4420	15 23 22.3 +44 20 38		F	H γ , H β , Mgb, H α
HS1547+4708	15 47 14.2 +47 08 45	18.4		H β , H α
HS1548+4555	15 48 07.4 +45 55 20	18.5		Mgb, H α
HS1611+4825	16 11 57.9 +48 25 35	18.1	A or F	H γ , H β , H α
HS1612+4505	16 12 45.5 +45 05 57	17.5	F?	H β , Mgb, H α
HS1626+5132	16 26 47.2 +51 32 05	18.0	A or F	H β , H α
HS1639+5103	16 39 43.1 +51 03 43	18.5	A	H γ , H α
HS1655+5209	16 55 56.6 +52 09 42	17.3	F or G	G $_{band}$, H γ , H β , H α
HS1657+5207	16 57 47.0 +52 07 33	19.5	F or G	H β , Mgb, H α
HS1721+5819	17 21 23.1 +58 19 51	16.1	G	G $_{band}$, H γ , FeI?, H β , Mgb

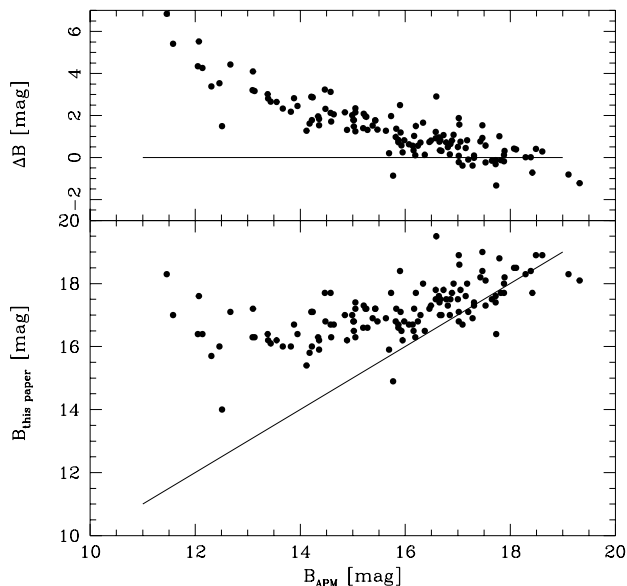


Fig. 6. The same as in Fig. 5 but for the comparison with the APM magnitudes.

case of extended objects, with $B \leq 16$, our survey is sensitive only for the emission core, the total magnitudes being thus systematically fainter.

4. The redshift distribution ranges between $0 < z < 0.1$, with a peak at $z=0.015$, which show that we found a sample of relatively nearby galaxies. The few galaxies with $z > 0.1$ were either selected as blue objects, or are Sy 1 galaxies.

Acknowledgements. We would like to thank Dr. A.P. Fairall for the careful review of this manuscript and Dr. Bernd Kuhn for observing some of our objects during his run in La Silla, December, 1994, as well as for his support with the reduction software. We gratefully acknowledge Dr. Dieter Engels for processing the magnitude calibration of the Hamburg prism plates. C. C. Popescu is greatly indebted to the astronomers from Hamburger Sternwarte for their warm hospitality during the work with their Plate Archive. It is a pleasure to thank the Calar Alto staff for their support during observations and Dr. Klaus Meisenheimer for his support during the Cafos22 run. U. Hopp acknowledge the support by Sonderforschungsbereich 375 of the Deutsche Forschungsgemeinschaft during the end of this project.

This research has made use of the NASA/IPAC Extragalactic Database (NED) which is operated by the Jet Propulsion Laboratory, California Institute of Technology, under contract with the National Aeronautics and Space Administration.

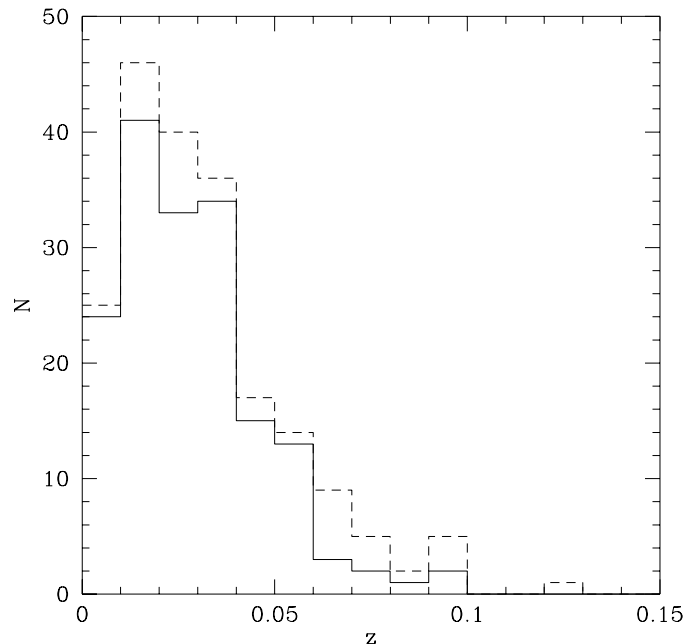


Fig. 7. The redshift distribution of our survey. With solid lines only the first priority objects are plotted, while with dotted lines all objects are included, also the second priority objects.

References

- Acker, A., Ochsenbein, F., Stenholm, B., Tylenda, R., Marcout, J., Schohn, C. 1992, The Strasbourg-ESO Catalogue of Galactic Planetary Nebulae, published by the European Southern Observatory
- Alonso, O., Zamorano, J., Rego, M. and Gallego, J. 1995, A&AS 113, 1
- Bardeen, J.M. 1986, in *Inner Space/Outer Space*, ed. E.W. Kolb, M.S. Turner, D. Lindley, K. Olive, and D. Seckel (University of Chicago Press, Chicago), p.212
- Binggeli, B., Tarenghi, M., Sandage, A. 1990, A&A 228, 42
- Bohuski, T.J., Fairall, A.P., and Weedman, D.W. 1978, ApJ 221, 776
- Clowes, R.G., Cooke, J.A., Beard, S.M. 1984, MNRAS 207, 99
- Cooke J.A., Beard, S.M., Emerson, D., Kelly, B.D., MacGillivray, H.T. 1986, MNRAS 219, 241
- Coziol, R., Demers, S., Peña, M., Torres-Peimberg, S., Fontaine, G., Wesemael, F., Lamontagne, R. 1993, AJ 105(1), 35 (Paper I)
- Coziol, R., Demers, S., Peña, M., Barnéoud, R. 1994, AJ 108, 405 (Paper II)
- Engels, D., Cordis, L., Köhler, T. 1994, in IAU Symposium 161, ed. H.T. MacGillivray, Kluwer, Dordrecht, p. 317
- Gallego, J. 1995, PhD thesis (Madrid)
- Hagen, H.-J., Groote, D., Engels, D., Reimers, D. 1995, A&AS 111, 195
- Haro, G. 1956, Bol. Obs. Tonantzintla y Tacubaya 14, 329

- 213, 971
- Horne, K. 1986, PASP 98, 609
- Hopp, U., and Kuhn, B. 1995, in *Astron. Ges. Review Ser.* 8, p. 277, ed. G. Klare
- Hopp, U., Kuhn, B., Thiele, U., Birkle, K., and Elsässer H. 1995, A&AS 109, 537
- Irwin, M., Maddox, S., and McMahon, R. 1994, RGO Spectrum 2, 14
- Irwin, M.J., and Trimble, V. 1984, AJ 89, 83
- Kaiser, N. 1986, in *Inner/Space/Outer Space*, see ref. Bardeen (1986), p.258
- Kibblewhite E.J., Bridgeland, M.T., Bunclark, P., Irwin, M. 1984, in: *Astronomical Microdensitometry Conference*, ed. D.A. Klinglesmith, NASA Conf. Pub. 2317, p. 277
- Kinman, T.D. 1984, in *Astronomy with Schmidt-Type Telescopes*, ed. M. Capaccioli (Dordrecht: Reidel), p. 409
- Kunth, D., Sargent, W.L.W., and Kowal, C. 1981, A&AS 44, 229
- Kunth, D. and Sargent, W.L.W. 1986, AJ 91, 761
- Maddox, S.J., Efsthathiou, G., Sutherland, W. and Loveday, J. 1990, MNRAS 242, 43
- Markarian, B.E. 1967, *Astrofizika* 3, 55
- Markarian, B.E., Lipovetskii, V.A., and Stepanian, D.A. 1983a, *Astrofizika* 19, 29; *Astrophysics* 19, 14
- Markarian, B.E., Lipovetskii, V.A., and Stepanian, D.A. 1983b, *Astrofizika* 19, 221
- Markarian, B.E., Lipovetskii, V.A., and Stepanian, D.A. 1984, *Astrofizika* 20, 419
- Maza, J., Ruiz, M.T., Gonzalez, L.E., and Wischnjewsky, M. 1989, ApJS, 69 (list 1)
- MacAlpine, G.M., Smith, S.B., and Lewis, D.W. 1977a, ApJS 34, 95 (List I)
- MacAlpine, G.M., Smith S.B., and Lewis, D.W. 1977b, ApJS 35, 197 (List II)
- MacAlpine, G.M., Lewis, D.W., Smith, S.B. 1977c, ApJS 35, 203 (List III)
- MacAlpine, G.M., Lewis, D.W. 1978, ApJS 36, 587 (List IV)
- MacAlpine G.M. and Williams, G.A. 1981, ApJS 45, 113 (List V)
- Metcalfe, N., Fong, R., Shanks, T. 1995, MNRAS 274, 679
- Moody, J.W., Kirshner, R.P., MacAlpine, G.M., and Gregory, S.A. 1987, ApJ 314, L33
- Pesch, P., Sanduleak, N. (Paper I) 1983, ApJS 51, 171
- Pesch, P., Sanduleak, N. (Paper III) 1986, ApJS 60, 543
- Pesch, P., Sanduleak, N. (Paper V) 1988, ApJS 66, 297
- Pesch, P., Sanduleak, N. (Paper VIII) 1989, ApJS 70, 163
- Pesch, P., Sanduleak, N., and Stephenson, C.B. (Paper XII) 1991, ApJS 76, 1043
- Pesch, P., Stephenson, C.B., and MacConnell D.J. 1995, ApJS 98, 41
- Salzer J.J. 1989, ApJ 347, 152
- Salzer, J., MacAlpine, G.M., and Boroson, T.A. 1989, ApJS 70,447
- Salzer, J., Moody, J.W., Rosenberg, J.L., Gregory, S.A., and Newberry, M.V. 1995, AJ 109, 2376
- Sanduleak, N. and Pesch, P. 1982, ApJ 258, L11
- Sanduleak, N., Pesch, P. (Paper II) 1984, ApJS 55, 517
- Sanduleak, N., and Pesch, P. (Paper IV) 1987, ApJS 63, 809
- Sanduleak, N., Pesch, P. (Paper IX) 1989, ApJS 70, 173
- Sanduleak, N., Pesch, P. (Paper XI) 1990, ApJS 72, 291
- Schneider, D.P., Schmidt, M., Gunn, J.E. 1994, AJ 107, 1245
- Smith, M.G. 1975, ApJ 202, 991
- Smith, M.G., Aguirre, C. and Zelman, M. 1976, ApJS 32, 217 (List N1)
- Stepanian, J.A., Lipovetsky, V.A., and Erastova, L.K. 1990, *Astrofizika* 32, 441; *Astrophysics* 32, 252
- Stepanian, J.A., Lipovetsky, V.A., and Erastova, L.K. 1991, *Astrofizika* 34, 205; *Astrophysics* 34, 99
- Stephenson, B., Pesch, P. (Paper XII) 1992, ApJS 82, 471
- Stickel, M., Fried, J.W., Kühr, H. 1993, A&AS 98, 393
- Surace, C. 1993, PhD thesis (Marseille)
- Surace, C., Comte, G. 1994, A&A 281(3), 653
- Takase, B., and Miyauchi-Isobe, N. 1988, *Ann. Tokyo Astr. Obs., Ser. 2*, 22, 41
- Thuan, T.X., Gott, J.R., Schneider, S.E. 1991, ApJ 315, L93
- Wamsteker, W., Prieto, A., Vitores, A., Schuster, H.E., Danks, A.C., Gonzalez, R., and Rodriguez, G. 1985, A&AS 62, 255
- Wasilewski, A.J. 1983, ApJ 272, 68
- Weistrop, D., Hintzen, P., Kennicutt, R.C., Liu, C., Lowenthal, J., Cheng, K.-P., Oliverson, R., Woodgate, B. 1992, ApJ 396, L23
- Wisotzki, L. 1994, in *IAU Symposium 161*, eds. H.T. MacGillivray et. al. (Kluwer, Dordrecht) 723
- Zamorano, J., Rego, M., González-Riestra, R., and Rodríguez, G. 1990, Ap&SS 170, 353
- Zamorano, J., Rego, M., Gallego, J., Vitores, A.G., González-Riestra, R., and Rodríguez-Caderot, G. 1994, ApJS 95, 387
- Zeldovich, Y.B., Einasto, J., and Shandarin, S.F. 1982, *Nature* 300, 407